



HAL
open science

New tectono-sedimentary evidences for Aptian to Santonian extension of the Cretaceous rifting in the Northern Chotts range (Southern Tunisia)

Mohamed Gharbi, Amara Masrouhi, Nicolas Espurt, Olivier Bellier, El Amjed Amari, Mohamed Ben Youssef, Mohamed Ghanmi

► To cite this version:

Mohamed Gharbi, Amara Masrouhi, Nicolas Espurt, Olivier Bellier, El Amjed Amari, et al.. New tectono-sedimentary evidences for Aptian to Santonian extension of the Cretaceous rifting in the Northern Chotts range (Southern Tunisia). *Journal of African Earth Sciences*, 2013, 79, pp.58-73. hal-01837215

HAL Id: hal-01837215

<https://amu.hal.science/hal-01837215v1>

Submitted on 27 Aug 2018

HAL is a multi-disciplinary open access archive for the deposit and dissemination of scientific research documents, whether they are published or not. The documents may come from teaching and research institutions in France or abroad, or from public or private research centers.

L'archive ouverte pluridisciplinaire **HAL**, est destinée au dépôt et à la diffusion de documents scientifiques de niveau recherche, publiés ou non, émanant des établissements d'enseignement et de recherche français ou étrangers, des laboratoires publics ou privés.

Accepted Manuscript

New tectono-sedimentary evidences for Aptian to Santonian extension of the Cretaceous rifting in the Northern Chotts range (Southern Tunisia)

Mohamed Gharbi, Amara Masrouhi, Nicolas Espurt, Olivier Bellier, El Amjed Amari, Mohamed Ben Youssef, Mohamed Ghanmi

PII: S1464-343X(12)00202-6

DOI: <http://dx.doi.org/10.1016/j.jafrearsci.2012.09.017>

Reference: AES 1804

To appear in: *African Earth Sciences*

Received Date: 18 April 2012

Revised Date: 21 September 2012

Accepted Date: 30 September 2012



Please cite this article as: Gharbi, M., Masrouhi, A., Espurt, N., Bellier, O., Amari, E.A., Youssef, M.B., Ghanmi, M., New tectono-sedimentary evidences for Aptian to Santonian extension of the Cretaceous rifting in the Northern Chotts range (Southern Tunisia), *African Earth Sciences* (2012), doi: <http://dx.doi.org/10.1016/j.jafrearsci.2012.09.017>

This is a PDF file of an unedited manuscript that has been accepted for publication. As a service to our customers we are providing this early version of the manuscript. The manuscript will undergo copyediting, typesetting, and review of the resulting proof before it is published in its final form. Please note that during the production process errors may be discovered which could affect the content, and all legal disclaimers that apply to the journal pertain.

1 **New tectono-sedimentary evidences for Aptian to Santonian extension of**
2 **the Cretaceous rifting in the Northern Chotts range (Southern Tunisia)**

3 Mohamed Gharbi^{a,b*}, Amara Masrouhi^{a,b}, Nicolas Espurt^b, Olivier Bellier^b, El Amjed Amari^a,
4 Mohamed Ben Youssef^c and Mohamed Ghanmi^d.

5 ^a Département des Sciences de la Terre, Faculté des Sciences de Gabès, Université de Gabès,
6 Cité Erriadh, 6072 Gabès, Tunisia

7 ^b Aix-Marseille Université, Institut Pytheas, CNRS, CEREGE UMR 7330, Aix-en-Provence,
8 France

9 ^c Centre de Recherches et Technologies des Eaux, BP 273, 8020 Soliman, Tunisia

10 ^d Département de Géologie, Faculté des Sciences de Tunis, 1060 Tunis, Tunisia

11 * *corresponding author; gharbim.mohamed@gmail.com phone: +216 75 392600; fax: +216 75*
12 *392421*

13 **Abstract**

14 Based on new structural, sedimentary, stratigraphic and seismic reflection data from
15 Cretaceous sequences of the Zemlet el Beidha anticline of the northern Chotts range (South
16 Tunisia), this study yields fresh insights into the geodynamic evolution of the South Tethyan
17 margin. The rifting of the margin started in the Triassic-Jurassic and continued during the
18 Aptian-Albian. In this last period N to NE trending extension was associated with WNW and
19 NW trending normal faults, bounding the developing horsts and grabens structures. This
20 tectonic framework is highlighted by strong thickness and facies changes in the Aptian-Albian
21 series associated with slumps and syntectonic conglomerates. During the Coniacian to
22 Santonian times, the study area was characterized by continued subsidence. Consequently, the
23 Coniacian-Santonian series are represented by sedimentary infilling consisting of post-rift
24 marl-rich sequences followed by limestone and marl sequences.

25 Folds geometry and associated faults system and tectonics analysis, confirm the role of
26 the Aptian-Albian rifting inheritance faulting in the structuring and the development of the
27 folds and thrusts belts of the southern Tunisian Atlas during the Cenozoic inversion, in
28 particular in the development of the ENE striking structures such as the Zemlet el Beidha
29 anticline.

30 **Keywords:**

31 South Tethyan margin, Rifting, Aptian-Santonian, Southern Atlasic domain, Tunisia, Chotts
32 range, Zemlet el Beidha anticline

33 **1. Introduction**

34 The geodynamic evolution of the northern margin of Africa has been studied by many
35 authors (Dercourt et al., 1986; Philip et al., 1986; Dewey et al., 1986; Soyer and Tricart, 1987;
36 Guiraud and Maurin, 1991; 1992; Martinez et al., 1991; Piqué et al., 2002; Bouaziz et al.,
37 2002; Burnet and Cloetingh, 2003), observing, that this margin was characterized by (1) the
38 extension, crustal stretching and thinning, as well as subsidence during the Mesozoic Tethyan
39 rifting (Bouaziz et al., 2002; Piqué et al., 2002; Bumby and Guiraud, 2005), and (2) the
40 occurrence of subsequent inversion during Late Cretaceous-Cenozoic subduction and
41 collision (Guiraud et al., 1991; Guiraud and Bosworth, 1997; Guiraud, 1998; Laville et al.,
42 2004; Abrajevitch et al., 2005; Bumby and Guiraud, 2005; Dhari and Boukadi, 2010).

43 Along the northern margin of Africa, the rifting began during the Late Permian-
44 Middle Triassic period (Raulin et al., 2011), and culminated at the transition between the
45 Triassic and Jurassic. The Early Mesozoic transgressions are characterized by a
46 heterogeneous sedimentary cover (Piqué et al., 2002; Courel et al., 2003; Guiraud et al.,
47 2005). During this sedimentation cycle an extensional tectonic context predominated, as
48 indicated by numerous synsedimentary normal faults systems. During the Jurassic time, a
49 regional extensional tectonic regime produced the dislocation of the existing continental

50 platform, which is related to the opening of the Central Atlantic and led to the development of
51 “*en échelon*” normal faults, tilted blocks and volcanic activity (Laridhi Ouazaa and Bédir,
52 2004). The distribution of the sedimentary facies has taken place along the WSW trending
53 Atlassic range from Morocco to northern Tunisia during the Late Liassic-Early Cretaceous
54 period (Piqué et al., 2002; Guiraud et al., 2005).

55 In southern Tunisia, the rifting has been associated with the development of WNW to
56 NW trending half grabens related to high rate subsidence, especially during Neocomian and
57 Barremian (Piqué et al., 1998; Bouaziz et al., 2002; Guiraud et al., 2005; Herkat et al., 2006).
58 The rifting led to presence of unconformities within many basins in the Early Aptian (Guiraud
59 and Maurin, 1991; 1992; Zouaghi et al., 2005b; Bodin et al., 2010) and continued during the
60 Aptian-Albian creating N to NE trending regional extension (Zghal et al., 1998; Rigane et al.,
61 2010). The Early Aptian unconformities mentioned above are associated with the lower
62 Cretaceous rifting stage. On the contrary, these later are related by some authors to the
63 compressional regime (Austrian Event; Ben Ayed, 1993; Bedir et al., 2001; Zouaghi, al.,
64 2005; Lazez et al., 2008) and/or halokinetic movements (Rigane et al., 2010; Zouaghi, al.,
65 2011).

66 Along the southern margin of Tunisia, the rifting has been associated with volcanism
67 in the Pelagian block (Fig. 1A; Ouazaa and Bédir, 2004). Extensional structures have been
68 recognized by surface and subsurface data in the Northern African margin (Piqué et al., 2002;
69 Bumby and Guiraud, 2005; Guiraud et al., 2005). The Cretaceous evolution of this margin
70 was associated with thickness and facies variations of the sedimentary sequences (Ben
71 Youssef et al., 1985; Ben Ferjani et al., 1990; Delteil et al., 1991; Abdallah et al., 1995;
72 Souquet et al., 1997; Bédir et al., 2001; Patriat et al., 2003; Zouaghi et al., 2005). This
73 tectonic regime involved the reactivation of pre-existing (Early Cretaceous) passive margin
74 structures, with a maximum extension occurring during Albian times. Early Cretaceous

75 extensional structures have been sealed by Senonian post-rift series with reefal buildings
76 along uplifted ridges (Negra et al., 1995). Thereafter, during Late Cretaceous and Cenozoic
77 times, tectonic inversion occurred as a result of convergence between Africa and Eurasian
78 plate. The North African margin was characterized by the reactivation of pre-existing
79 extensional faults systems which controlled fault-related folds (Zargouni, 1985; Ben Ayed,
80 1986; Catalano et al., 1996; Doglioni et al., 1999; Vergés and Sabat, 1999; Frizon de Lamotte
81 et al., 2006; Masrouhi et al., 2007; Dhahri and Boukadi, 2010).

82 This study focuses on the structure of the Zemlet el Beidha anticline in the eastern part
83 of the northern Chotts range, which belongs to the southern Atlassic front of Tunisia. In this
84 area, the tectono-sedimentary framework displays evidence for the southernmost Cretaceous
85 rifting. Our study provides new structural elements, new detailed geologic mapping,
86 sedimentologic, palaeontologic and new interpretation of geophysical data to understand the
87 Cretaceous passive margin evolution.

88 **2. Geological setting**

89 *2.1. Structural features of the study area*

90 The Atlas orogen forms a part of the present-day North African margin and is the
91 result of the collision between the African and the European plates. The development of the
92 southern Tunisian Atlas fold-and-thrust belt is related to this tectonic convergence occurred
93 during Tertiary times. This domain is characterized by E-W to NE-SW and NW-SE anticlines
94 separated by synclines filled with Neogene and Quaternary series (Fig. 1B; Zargouni, 1985;
95 Abdeljaoued and Zargouni, 1981; Burollet, 1991; Bédir et al.; 2001, Hlaim, 1999; Bouaziz et
96 al, 2002).

97 The southern Tunisian Atlas fold-and-thrust belt is limited westward by major NW
98 trending strike-slip fault systems (Gafsa and Negrine-Tozeur fault systems; Fig. 1A, B). The

99 Gafsa fault system (Zargouni, 1984; Burollet, 1991; Haleim, 1999) is a N120° E trending
100 dextral strike-slip system (Zargouni et al., 1985; Abbès and Zargouni, 1986; Abbès et al.,
101 1994; Boutib and Zargouni, 1998) and cuts the Bou Ramli, Ben Younes and Orbata anticlines
102 in the north and the Zemlet el Beidha and Koudiat Hammamet anticlines in the south (Fig.
103 1B, C). Another prominent northwest striking strike-slip fault is the Negrine-Tozeur fault
104 (Fig. 1B), which borders the west of the Gafsa-Metlaoui basin and parallel to the Gafsa fault.
105 It extends from the Negrine (Algeria) through the Tunisian Atlas Mountains (Zargouni, 1984;
106 Zargouni et al., 1985). The Sehib, Berda, Chemsî and Belkheir folds separate the wide Gafsa-
107 Metlaoui basin to the northern Chotts range towards the south.

108 The Chotts depression corresponds to foredeep depozone (according to the
109 nomenclature of DeCelles and Giles, 1996). This foredeep depozone is formed by two
110 connected depression: the Chott El-Jérid to the west and the Chott El-Fejej to the east (Fig.

111 1B, C). The Chott El-Fejej occupies the core of a mega-anticline called “Fejej dome” whose

112 southern limb corresponds to Jebel Tebaga and northern limb is formed by the northern
113 Chotts range (Fig. 1B, C).

114 The eastern part of the northern Chotts range fold belt is affected by several faults
115 that's the most significant is the Bir Oum Ali and Fejej faults system (Fig. 1B). The northern
116 Chotts range (E-W trend) changes direction to a NE-SW in its eastern part that corresponds to

117 the Zemlet el Beidha anticline. The Zemlet el Beidha anticline limits the Sidi Mansour basin
118 in the north and the Chotts Fejej basin in the south (Fig. 1C). The Zemlet el Beidha anticline
119 (Fig. 2) belongs to the southern Atlassic front of Tunisia in the eastern part of the northern
120 Chotts range (Fig. 1B). It is located between an intensely deformed domain, the southern
121 Atlassic fold-and-thrust belt, in the north, and a less deformed domain, the Saharan Platform,
122 in the south (Fig. 1A, B), (Zargouni, 1984; Ben Ferjani et al., 1990; Burollet, 1991; Haleim,
123 1999; Bouaziz et al., 2002).

124 2.2. General stratigraphy

125 The stratigraphy (Fig. 3) of the Zemlet el Beidha region is derived from
126 micropaleontology analysis (Table. 1) and from boreholes which were drilled close to the
127 anticline (wells 1, 2, 3 and 4, Fig. 1 C). The sedimentary series outcropping in the study area
128 are Cretaceous to Quaternary in age (Fig. 1C, 2 and 3). The core of the Zemlet el Beidha
129 anticline (Fig. 2) is formed by Hauterivian-Barremian marls, alternating with anhydrites,
130 limestones and claystones of the Bouhedma Formation (Abdejaouad and Zargouni, 1981;
131 Lazez and Ben Youssef, 2008). The Bouhedma Formation is overlain by shale-rich sands and
132 ferruginous sandstones of the Sidi Aïch Formation, for which a Barremian (pro parte) age is
133 deduced from its stratigraphic position. The Sidi Aich Formation is overlain by the dolomitic
134 bank of the Lower Aptian Orbata Formation (Ben Youssef and Peybernes, 1986; Chaabani
135 and Razgallah, 2006), which is topped by a rich-Orbitolinidae hardground, showing some
136 Ammonites (Gharbi, 2008). This massive dolomitic bank is a common feature all over the
137 area and forms the flanks of folded structures. The Upper Albian deposits correspond to the
138 lower member of the Zebbag Formation. This formation, which rarely outcrops in the study
139 area, is dominated by dolomitic sandstones, marls, limestones and argillaceous limestones.
140 The upper member of Zebbag Formation (Upper Cenomanian-Turonian) is characterized by

141 the flint dolomitic bank of the Guettar member. This sequence is only deposited at Jebel
142 Jerouala (Fig. 2). The Coniacian-Santonian series of the Aleg Formation unconformably
143 overlie the previous series. They are defined by thick sequences of dolomitic sandstones at the
144 base and interbedded green marls and bioclastic limestones at the top. The fauna of this
145 formation is distinguished (Fig. 3 and Table. 1) by the ammonites in the Khanguet Aïcha
146 River, planktonic foraminiferas in the Gouada plain and the Rudistes in the Khanguet Telmem
147 (Abbès and Tlig, 1991; Louhaïchi and Tlig, 1993; Gharbi, 2008). The Abiod Formation
148 conformably overlies the Aleg Formation and consists of limestone banks with intercalations
149 of thin clay layers. These intercalations are enriched by phosphatic debris and glauconite
150 grains. The associated fauna suggests a deep marine environment, similar to the central and
151 northern Tunisian domain (Abdeljaouad and Zargouni, 1981). According to facies (Louhaïchi
152 and Tlig, 1993) and microfauna data (Gharbi, 2008), the Abiod Formation is Upper
153 Campanian to Maastrichtian in age (Fig. 3 and Table. 1).

154 The Cenozoic series of the study area are composed by thin Paleocene marine marls
155 covered by Paleogene and Neogene continental sediments. The Early Tertiary comprises
156 green clays of the El Haria Formation. The clays show a Maastrichtian to Paleocene marine
157 fauna (Gharbi, 2008). The Bouloufa Formation is dated to the Middle Eocene by Abdeljaouad
158 (1987) and overlies unconformably (U1) the clays of the El Haria Formation. It is formed by
159 red gypsum clay and encrusted limestone with *Bulimes* fauna. At the end of Eocene period,
160 south and central Tunisia emerged and compressional deformations took place (Masrouhi et
161 al., 2008; Frizon de Lamotte et al., 2009). As a result, intense erosion in the Atlassic fold-and-
162 thrust belt zone caused the deposition of thick syntectonic series of silt and molasse basins
163 during the Neogene and Quaternary. Miocene sands of the Beglia Formation unconformably
164 overlie (U2) the Bouloufa Formation. Finally, the Segui Formation, which crops out on the
165 southern flank of the Zemlet el Beidha anticline, consists of coarse alluvial conglomerate

166 deposits. The Segui Formation unconformably overlies (U3) the Beglia Formation and record
167 the growth of the Zemlet el Beidha anticline.

168 **3. Zemlet el Beidha Cretaceous structures**

169 *3.1. Structures*

170 The Zemlet el Beidha structure corresponds to a south-verging asymmetric thrust-
171 related anticline with a curved axis that changes from an E strike to NE strike from west to
172 east (Fig. 2). The Zemlet el Beidha anticline has a single periclinal closure in the east. As
173 shown in geologic map of Figure 2, the core of the Zemlet el Beidha consists of Coniacian-
174 Santonian outcrops in the Jebel Romana and Gouada plain (NE part of Zemlet el Beidha).
175 Westward, the anticline of Jebel Haidoudi is occupied by the Coniacian-Santonian deposits.
176 In the central part, the core of the anticline is formed by the Hauterivian-Barremian series.

177 The geometry of the Zemlet el Beidha anticline is illustrated by the two cross sections
178 of Figure 4. The section A-A' crosses the eastern part of the anticline (Fig. 2 and 4). In the
179 Tebaga Fatnassa region, the fold corresponds to a gently deformed anticline of Cretaceous
180 strata unconformably overlain by Late Miocene (U2) and Late Pliocene to Quaternary series
181 (U3). The northern backlimb is formed by $\sim 10^\circ$ N-dipping thin layers of marls (Fig. 4A),
182 alternating with anhydrites, limestones and claystones of the Bouhedma Formation. The series
183 are also deformed by the N-dipping normal faults. The southern forelimb is formed by
184 Coniacian-Santonian series of the Aleg Formation and dips $\sim 20^\circ$ southeastward. The central
185 part, the Khanguet Aïcha and Khanguet Amor region, exposes a forelimb formed by \sim almost
186 45° S-dipping layer (Fig. 2 and 5). The southern flank of the Zemlet el Beidha anticline also
187 shows subvertical faults, previously interpreted by several authors as strike-slip faults
188 (Abdeljaouad and Zargouni, 1981; Zargouni et al., 1985; Abbès and Zargouni, 1986; Abbès et
189 al., 1986).

190 Along the cross section B-B' (Fig. 4), the northern limb of the anticline exhibits 5-10°
191 N-dipping Hauterivian-Barremian series. The cross section B-B' shows a Cretaceous series
192 from the Hauterivian to Late Maastrichtian unconformably overlain by Middle Eocene, Late
193 Miocene and Late Pliocene to Quaternary (U1, 2, 3) series on the Jebel Jerouala and Jebel
194 Haidoudi (Figs. 2 and 4). The western part of the Zemlet el Beidha anticline is characterized
195 by a 70°-80° S-dipping forelimb intensively deformed by the S-vergent faults acting now as
196 right-lateral oblique-slip of the Fejej corridor (Fig. 2).

197 3.2. Fault kinematics analysis

198 The Zemlet el Beidha area has undergone a complex tectonic evolution related to its
199 geometric position in relation to the whole northern Chotts range. To support our structural
200 interpretation we measured and analyzed striated fault planes within Aptian-Albian series.
201 Such a fault kinematics analysis of mesoscale faults permits a quantitative reconstruction of
202 paleostresses that can be related to the chronological sequence and orientations of larger-scale
203 structures. These paleostresses thus provide useful information not only on the compressional,
204 extensional or strike-slip origin of larger structures, but also on their kinematics and
205 orientation relative to the stress field (oblique or normal).

206 The western part of the Zemlet El Beidha anticline (Jebel Haidoudi, Jebel Fejej and
207 Jebel Jerouala) is characterized by a major NW to WNW-trending fault Fejej system
208 (Abdeljaouad and Zargouni, 1981; Zargouni et al., 1985; Abbès and Tlig, 1991; Louhaïchi
209 and Tlig, 1993). This fault system, acting now with a right-strike-slip component, may
210 correspond to inherited Cretaceous normal faults (Gharbi, 2008). The detailed geologic
211 mapping (1:25 000) of the Khanguet Aïcha area (central part of Zemlet el Beidha, Fig. 2)
212 combined with the SPOT images (Fig. 5A, B) also show numerous N100-110° E apparent
213 trending strike-slip faults. These faults are well expressed in the southern flank of the Zemlet

214 el Beidha anticline. The Khanguet Aïcha and the Khanguet Amor faults appear on map as
215 strike-slip faults. They affect the Hauterivian to Albian series and are sealed by Coniacian-
216 Santonian deposits (Fig. 5B, C) with no evidence of recent displacement (Fig. 5 and 6). Fault
217 kinematics analysis performed along the Khanguet Aïcha and Khanguet Amor faults (Fig.
218 5D) shows oblique strike-slip faulting component. The normal faulting generates the
219 sedimentary reworking of the Aptian dolomitic bank in the Khanguet Aïcha and Khanguet
220 Amor. The syntectonic Aptian conglomerates (Fig. 7 A, B, C and D) observed in the
221 downdropping normal fault of Khanguet Aïcha and Khanguet Amor (Fig. 6) indicated tilted
222 block geometry. In addition, the eastern part of Tebaga Fatnassa (Fig. 2) exposes growth
223 strata in the hanging-wall of the ancient normal fault testifying the Albian extensional regime
224 (Fig. 8).

225 Using the fault diagram, we rotated the fault data to restore the bedding plane to its
226 horizontal orientation. The resulting back-tilted fault diagram shows that these faults were
227 normal faults before Cenozoic tilting (Fig. 5D). This pre-tilting normal faulting shows a ~NE
228 trending extension (Fig. 5D). The reactivation of this normal fault is attested by reverse sense
229 of movement (Fig. 8) and shows thrust reactivation and the shortcut geometry affecting the
230 Bouhedma Formation in the core of the Zemlet el Beidha anticline (Fig. 9).

231 3.3. *Tectono-sedimentary data*

232 Along-strike correlation of the sedimentary sequences of the Zemlet el Beidha region
233 allows us to characterize at least four periods of tectono-sedimentary evolution related to the
234 Cretaceous rifting (Fig. 10A) i.e. Neocomian, Aptian-Albian, Coniacian-Santonian and
235 Campanian-Maastrichtian tectono-sedimentary sequences.

236 During the Neocomian, a sporadic clastic sedimentation testifies two periods of marine
237 regression. The sequences correspond essentially to continental sediment including sands,

238 clays, silts, lacustrine dolomites and gypsum deposits. The Early Albian tectonic extensional
239 episode is recorded by N100-110° E trending faults related to a regional N to NE trending
240 extension. This tectonic episode may be associated with the general uplift and erosion (ds1) of
241 the Zemlet el Beidha zone (Fig. 10A) and continued to Early Albian times. The subsidence in
242 the northern Chotts range area began during the Hauterivian-Barremian. Sedimentary features
243 such as small slumps (Fig. 11 A), turbidites, mudflows (Fig. 11 B), and several meter scale
244 olistoliths (included within the Barremian anhydrites, limestones and claystones) indicate
245 basin instabilities. The Early Aptian dolomitic series include rare orbitolines and ammonites
246 (Fig. 11 C; Abdeljaouad and Zargouni, 1981; Ben Youssef and Peybernès, 1986; Chaabani
247 and Razgallah, 2006; Lazez et al., 2008; Gharbi, 2008) give evidence for a hard ground
248 surface. In the Khanguet Aïcha, this dolomitic bank is also affected by the N110°E trending
249 faults. This faulting is associated with thickness and facies variations of the Barremian series
250 (Fig. 5C) as well as the occurrence of Aptian conglomerates within the hanging-walls of the
251 Kanguet Aïcha and Kanguet Amor faults (Figs. 5 and 6). These conglomerates probably attest
252 to syntectonic sedimentation during normal faulting. Moreover, the stratigraphic correlation
253 of Fig. 10A shows usually lateral thickness changes from the Khanguet Amor (log 7) to the
254 Kanguet Aïcha (log 8) areas that appear to be correlated with the normal faults. The Early
255 Aptian tectonic extensional episode is well known in the northern Chotts range and south
256 Atlassic domain. It is characterized by a tilted block system associated with horsts and
257 grabens. In fact, this structural frame is responsible for the distribution of the Albian
258 sequences in the northern Chotts range and the regional unconformity deposits which are
259 defined by the absence of the deposits of Late Aptian and of the Early and Middle Albian age
260 (Abdeljaouad and Zargouni, 1981; Ben Youssef et al., 1984; Lazez et al., 2008).

261 In this area, the irregular distribution of these series is also expressed within deposits
262 around the uplifted zone of the present-day Zemlet el Beidha fold (Fig. 10B). In this region,

263 the series distribution is related to a tilted bloc geometry, which has been dated to the
264 Neocomian-Early Albian. Faulting produced differential uplift and high subsidence rates in
265 the northeastern Chotts range (Fig. 10B).

266 The transgressive Cenomanian and Turonian period is well known across the northern
267 African plate. Despite this transgression (Guiraud et al., 2005), the tectonic activity induced
268 differential subsidence; the Zemlet el Beidha formed an uplift zone during this period of high
269 sea level. The Jebel Jerouala is the unique locality (log 3 in Fig. 10A) where Turonian
270 sediments were deposited. In this zone we note the presence of red flint dolomite limited by
271 the Fejej normal fault systems. The thickness variations and the main tectonic elements
272 suggest that the Turonian sedimentation was controlled by WNW to NW trending faults.

273 The Coniacian-Santonian sedimentation is characterized by a subtle onlap pattern and
274 facies changes. These sediments consist of marl-rich limestones and clays enriched by benthic
275 and pelagic foraminifera and ostra, indicating a deepening basin. On the northern side and
276 southern flank of the Zemlet el Beidha anticline, the strong thickness of the Coniacian-
277 Santonian series is related to the reactivation of NW trending faults that delimited the Zemlet
278 el Beidha horst (Fig. 2 and 10A). Eastward, the region of Gouada plain (Fig. 2) is
279 characterized by pelagic facies (Fig. 10A) while westward, at Jebel Haidoudi, the deposits are
280 characterized by benthic facies. In the Khanguet Telmem (Fig. 2 and log 5 and 6 in Fig. 10A),
281 a lens of reef-building rudist colonies (Fig. 11D) has been observed, which recorded and
282 developed due to the Zemlet el Beidha uplift. The rudist coral limestones preferentially
283 developed on the horst of Zemlet el Beidha. During the Coniacian-Santonian stage, the
284 paleostructure of the Zemlet el Beidha limits SW and NE marginal zones with basin
285 sedimentation. In particular, the eastern Tebaga Fatnassa-Gouada plain and the western Jebel
286 Fejej-Haidoudi area are characterized by strong subsidence during the Coniacian-Santonian

287 (log 1, 2, 9, 10 in Fig. 10A). This subsidence is consistent with the previous tectonic context
288 described above.

289 During the Campanian, the western part of the Zemlet el Beidha domain is
290 characterized by marine transgression, recorded by the occurrence of deepwater limestones
291 and clays, and pelagic facies in the Late Campanian. West of the Zemlet el Beidha area, just
292 at the south of Jebel Fejej (Fig. 2 and Fig. 10 log 1, 2 and 3) and on the Jebel Haidoudi, these
293 series are transgressive, and a significant increase in thickness subsidence rate is recorded by
294 the Late Maastrichtian series. In the Fejej graben, the structural evolution during the
295 Campanian and Late Maastrichtian led to a significant subsidence increase as a consequence
296 of the transtensional (Guiraud et Bosworth, 1997; Zouari et al., 1999) displacement of the
297 Fejej fault.

298 **4. Discussion: Geodynamic evolution of the southern Atlasic margin**

299 *4.1. Cretaceous rifting inheritances*

300 4.1.1. Aptian-Albian syn-rift

301 The northern Chotts range was dominated by regional normal faulting. The WNW and
302 NW trending faults were mainly inherited from the Jurassic and reactivated during the Early
303 Cretaceous-Albian times (Gharbi, 2008). Seismic reflection profiles of Figure 12 illustrate the
304 structural architecture of the southern Tethyan margin in the northern Chotts range. Analysis
305 of the seismic profiles EL05 and EL07 crossing the Sidi Mansour Basin (Fig. 1C) permits to
306 identify faults with normal components bounding the subsiding domains (Fig. 12). These
307 faults are associated with other synthetic faults that have contributed to the formation of a
308 major graben systems. The study area is marked by thick Hauterivian-Barremian and Albian
309 deposits, which are progressively thickening, associated with listric faults (Fig. 12). The

310 geometry and the thickness variations are interpreted to be related to the regional extensional
311 strain during the Aptian-Albian. The evolution proposed in Fig.13 shows a possible tectonic
312 scenario for the Zemlet el Beidha zone during Aptian-Albian faulting. The reactivation of the
313 Khanguet Aïcha fault is associated with syntectonic conglomerates and leads to produce an
314 unconformity at the base of the Upper Aptian series (Fig. 3, log 5, 8 in Fig. 10A and B, Fig.
315 13). Our observations suggest that this unconformity is associated with normal faults and an
316 extensional tectonic regime. Such as the Jebel Chemsî, Jebel Bir Oum Ali at west of Zemlet el
317 Beidha, Jebel Tebaga of Kebili (Fig. 14 a, b and c), the fault kinematics deduced from the
318 study of striated fault planes display evidence for the tectonic regime which is extensional
319 during the Aptian-Albian period. Geologic and geophysic data were integrated to confirm that
320 the syn-rift tectonic in the northern Chotts range is still related to the Early Albian. This
321 rifting has been accompanied by an episode of volcanism which is testified by basalt flows
322 observed in the pelagian blocks of eastern Tunisia (Fig. 1B; Ellouz et al., 2003; Ouazaa and
323 Bédîr, 2004).

324 Many interpretations have been proposed to explain the Upper Aptian-Lower Albian
325 regional unconformity. Several authors interpret this unconformity as the result of a major
326 compressional event during the Aptian-Albian time (the Austrian Phase, Ben Ayed, 1993;
327 Bédîr et al., 2000; Bouaziz et al., 2002; Zouaghi et al., 2005). Other authors plead for an
328 extensional event (normal faulting regime) (Martinez et al., 1991; Guiraud, 1998; Zghal et al.,
329 1998; Zouari et al., 1999; Guiraud et al., 2005; Bodin et al., 2010; Rigane et al., 2010). Our
330 observations yield fresh data to support an Aptian-Albian extensional deformation of the
331 south Tethyan margin. This rifting episode ended with a regional unconformity identified by a
332 hard ground surface, and halokinetic movements (Bédîr et al., 2001; Rigane et al., 2010;
333 Zouaghi et al., 2011). Thus, the Upper Aptian-Lower Albian unconformity can be related to
334 intraplate extensional deformation linked to the opening of the central segment of the South

335 Atlantic while the northward movement of part of the African Plate was accompanied by N
336 trending extension registered in the central African basins (Martinez et al., 1991; Guiraud and
337 Maurin, 1991; Guiraud et al., 2005) and northeastward movement of the Arabian–Nubian
338 block during the Aptian–Albian transition (Bodin et al., 2010).

339 4.1.2. Coniacian-Santonian post-rift

340 The Coniacian-Santonian stage is attested by thick deposits of pelagic and benthic
341 facies (Fig. 10A). These deposits are characterized by thickness and facies variations and by
342 reefal carbonates on horst structures (log; 5, Fig. 10A). In Sidi Mansour Basin, the Coniacian-
343 Santonian sequence observed in seismic profile (EL-05, Fig. 12) shows along-strike changed
344 in term of thickness which does not follow the usual hierarchies of the Early Cretaceous
345 sequences. The ancient normal fault systems controlled the distribution of the Coniacian–
346 Santonian deposits that are marked by a significant thickness and facies variations from
347 northwest to southeast (Fig. 12). The Coniacian–Santonian distribution of the sedimentary
348 deposits testifies for a post rift stage with major transgression (Abdallah and Rat, 1987;
349 Herkat and Guiraud, 2006).

350 During the Coniacian-Santonian, the Maghreb area was covered by an important
351 transgression leading to a very extensive marine incursion covering the northern platforms of
352 the Sahara domain corresponding to shallow sea characterized by the deposition of a
353 homogeneous carbonate platform (Zouaghi et al., 2005; Herkat and Guiraud, 2006; Frizon de
354 Lamotte et al., 2009). A subsiding deep-marine basin has been developed in the Aurès
355 (Herkat and Guiraud, 2006) that allows the deposition of black deep-marine shales in the
356 Tunisian Atlas, which is one of the most important hydrocarbon-source rocks of the Atlas
357 system (Bédir et al., 2001; Zouaghi et al., 2005; Frizon de Lamotte et al., 2009).

358 4.1.3. Campanian-Maastrichtian tectonic reactivation

359 Several authors have suggested tectonic inversion in the Tunisia Atlas since the
360 Campanian (Guiraud and Bosworth, 1997; Guiraud et al., 2005; Herkat and Guiraud, 2006;
361 Masrouhi et al., 2008; Frizon de Lamote et al., 2009; Masrouhi and Koyi, 2012). Zouari et al.
362 (1999) defined that the inversion occurred between middle Turonian and the Late
363 Maastrichtian. In our study area, Late Campanian to Paleocene series are absent in the eastern
364 Zemlet el Beidha region. However, these series develops westward in the Fejej corridor (Fig.
365 2 and Fig. 10A). We propose that fault reactivation occurred during Late Campanian to
366 Paleocene, producing the westward migration of the subsidence from the Gouada plain to the
367 Fejej corridor (Fig. 10A). This tectonic event may be related to N trending compression which
368 reactivated the major inherited fault. This stage corresponds to southwestward migration of
369 the subsidence in the southern Atlasic domain, especially in the Gafsa Basin (Zouari et al.,
370 1999).

371 4.2. Implications for Cenozoic tectonic evolution

372 In this study, field data show evidences for unconformities and syntectonic deposits
373 recording several periods of shortening during the Cenozoic. We present here the sedimentary
374 signatures of the different pulses of shortening associated with the development of the Zemlet
375 el Beidha fold.

376 According to the cross section A-A' (Fig. 4), the unconformity angle between the
377 Coniacian-Santonian and the erosional Late Miocene surface is 10° while between Coniacian-
378 Santonian and Late Pliocene-Quaternary is about 20°. Locally south of the Jebel Jerouala, we
379 observed that the Late Middle Eocene unconformably overlie the Late Maastrichtian-
380 Palaeocene series (cross section B-B', Fig. 4). This unconformity confirms that the Zemlet el
381 Beidha Cretaceous basin was inverted during the Cenozoic. During the compressional

382 deformations, some extensional structures were not reactivated (Fig. 2 and Fig 4) while others
383 were reactivated and evolved to strike-slip faults, such as the apparent Khanguet Aïcha and
384 Khanguet Amor strike-slip faults (Fig. 5 and Fig. 6) and reverse faults (Fig. 8).

385 In addition, some Atlassic folds are related to the early halokinesis during Jurassic and
386 Early Cretaceous associated with the synsedimentary activity of some normal faults (Rigane
387 et al., 2010). The seismic lines interpreted by several authors (e.g., Hlaiem, 1999; Frizon de
388 Lamotte et al., 2000; 2009) show that the fold structures are associated with reverse deep-
389 seated faults rooting at depth within the Triassic levels. The position and orientation of pre-
390 existing structures would be related to the position of ancient normal faults which may be
391 probably linked to structural inheritance due to the Triassic-Jurassic to Aptian-Albian rift

392 (Guiraud, 1998; Guiraud et al., 2005). In our study area, the Upper Aptian-Albian normal
393 faulting also played a major role during Cenozoic compressions in controlling the structural
394 architecture of the Zemlet el Beidha anticline and probably, of others structures of the Chott
395 range.

396 **5. Conclusion**

397 The structural and tectono-sedimentary study of Jebel Zemlet el Beidha underlines the
398 predominant role of inherited structures acquired during the evolution of the southern Tethyan
399 margin, and their influence of the present-day geometry of the Atlassic fold belt. The
400 geodynamic history of the Tethyan margin during the Cretaceous in the northern Chotts range
401 can be divided into three different tectonic events. The first syn-rift Aptian-Albian period
402 shows a general episode of variable depositional thickness and facies variations. It is

403 dominated by an extensional stress regime. The onset of the tilted blocks along the N100-
404 110°E trending normal fault was associated with Upper Aptian syn-depositional
405 conglomerates. This extensional tectonics was also accompanied, in several regions of the
406 Atlas, by volcanic activity and halokinetic movement. The second Coniacian-Santonian
407 period corresponds to a post-rift stage with major marine transgression. The Coniacian-
408 Santonian extensional faulting is recognized in the southern Tunisian Atlassic domain. In
409 contrast, in Algeria and Morocco, the Coniacian-Santonian is characterized by the first period
410 of inversion tectonics (Herkat and Guiraud, 2006; Frizon de Lamotte et al., 2009). In our
411 study area, we propose that fault reactivation occurred during Late Campanian to Paleocene,
412 producing the westward migration of the subsidence. This tectonic event can be correlated
413 with the onset of the Africa-Eurasia convergence (Guiraud and Bosworth, 1997; Zouaghi et
414 al. 2005; Frizon de Lamotte et al., 2009). Major structural inversion of the Upper Aptian-
415 Albian normal faults occurred during successive Cenozoic compressions. This Cretaceous
416 inheritance controlled the structural architecture of the Zemlet el Beidha anticline and
417 probably of others structures of the Chott range.

418 **Acknowledgments**

419 This work is based on M. Gharbi's Masters at "Faculté des Sciences de Tunis"
420 (Tunisia) and PhD research at "University of Sfax", "Unité de Recherche Hydrosiences
421 Appliquées à Gabés (06/UR/10-03)" (Tunisia) and at CEREGE (Université Paul Cézanne
422 Aix-Marseille (UPCAM), France). M. Gharbi benefits of a Foreign Affair Ministry (Ministère
423 des Affaires Etrangères) grant through French Embassy in Tunisia and a complement support
424 through the "Cotutelle de thèse" program (F2IR program - UPCAM). Field has benefited
425 from financial support under UPCAM RFQ's International Relations. SPOT images were
426 provided thanks to the ISIS program (©CNES, distribution SPOT images S.A.). The Tunisian
427 Enterprise for Petroleum Activities (ETAP) and particularly A. Amri and Y. Bouazizi are

428 thanked for providing access to the seismic lines. We are indebted to Nick Marriner and Rita
429 Katharina Kraus for comments and English language corrections. We are grateful to Dr. W.
430 Bosworth and the anonymous reviewer for providing constructive reviews that significantly
431 improved this article.

432 **References**

- 433 Abbès, A. et Tlig, S., 1991. Tectonique précoce et sédimentation de la série Crétacée dans le
434 bassin des Chotts (Tunisie du sud) Géologie Méditerranéenne. Tome XVIII, n° 3. pp, 149-
435 161.
- 436 Abbès, C et Zargouni, F., 1986. Anatomie d'un couloir de décrochements: le couloir de
437 Hadifa (Chaîne Nord des Chotts-Tunisie). Rev. Sc. de la Terre, Vol. 4, Tunisie.
- 438 Abbès, C., Abdeljaouad, S. et Ben Ouezdou, H. 1986. Carte Géologique d'El Hamma au
439 1/100.000, feuille n°74. Institut National de recherche Scientifique de Tunisie et Service
440 Géologique Nationale d'Office Nationale de Mines, Tunisie.
- 441 Abdallah, H. et Rat, P., 1987. Le rôle de la faille de Gafsa dans le jeu transgressif et régressif
442 au Crétacé supérieur de la chaîne nord des Chotts (Tunisie). In Colloque: Transgressions et
443 régressions au Crétacé (France et régions voisines), Dijon, 1985 (ed. Saloman, J.), Mémoires
444 Géologiques de l'Université de Dijon 11. pp, 232–242
- 445 Abdallah, H., Memmi L., Damotte, R., Rat, P. and Magniez, Jannin F., 1995. Le Crétacé
446 supérieur de la chaîne Nord des Chotts (Tunisie du centre-sud): Biostratigraphie et
447 comparaison avec les régions voisines. Cretacous Research, 16. P,487-538.
- 448 Abdeljaouad, S et Zargouni, F., 1981. Mise en évidence d'une tectonique intracrétacé dans le
449 secteur de J. Zemlet El Beïda (chaîne des Chotts). Acte de 1er Congr. Nat. Sc. Terre, Tunis, t.
450 I, p, 285.

- 451 Abdeljaouad, S., 1987. Sur l'âge Paléocène supérieur-Miocène des dépôts continentaux à
452 calcrètes ou dolocrètes de la Formation Bouloufa en Tunisie méridionale. Conséquences
453 paléogéographiques. Bull. Soc. Géol. Fr, (8), t, III, n°4. pp, 777-781.
- 454 Abrajevitch, A.V., Jason, R.A., Aitchison, J.C., Badengzhu, Davis, A.M., Jianbing Liu, J., and
455 Ziabrev, S.V., 2005. Neotethys and the India–Asia collision: insights from a palaeomagnetic
456 study of the Dazhuqu ophiolite, southern Tibet. Earth and Planetary Science Letters 233. pp,
457 87-102.
- 458 Aris, Y., Coiffait, P.E., Guiraud, M., 1998. Characterization of Mesozoic–Cenozoic
459 deformations and paleostress fields in the Central Constantinois, northeast Algeria.
460 Tectonophysics. 290. pp, 59-85.
- 461 Bédir, M., Boukadi, N., Tlig, S., Ben Timzal, F., Zitouni, L., Alouani, R. Slimane, F., Bobier,
462 C., and Zargouni, F., 2001. Subsurface Mesozoic basins in the central Atlas of Tunisia,
463 tectonics, sequence deposit distribution and hydrocarbon potential, AAPG Bull. 85, 5. pp,
464 885-907.
- 465 Ben Ayed, N., 1986. Evolution tectonique de l'avant-pays de la chaîne alpine de la Tunisie du
466 début du Mésozo à l'Actuel. Thesis es-sciences, Univ. Paris Sud, Orsay, 347 p.
- 467 Ben Ferjani, A., Burollet, P., F. and Mejri, F. 1990. Petroleum geology of Tunisia. Entreprise
468 Tunisienne d'activités pétrolières, 194p.
- 469 Ben Youssef, M., Biely, A., et Memmi, L., 1985. La Formation Orbata (Aptien) en Tunisie
470 méridionale précisions biostratigraphiques nouvelles. Notes service géologique de Tunisie,
471 n°51. pp, 105-120.
- 472 Ben Youssef. M et Peybernes. B., 1986. Données micropaléontologiques et
473 biostratigraphiques nouvelles sur le Crétacé inférieur marin du Sud tunisien, J. Afr. Earth Sci.
474 5. pp, 217-231.

- 475 Bodin. S., Petitpierre. L., Wood. J., Elkanouni. I., and Redfern. J., 2010. Timing of early to
476 mid-cretaceous tectonic phases along North Africa: New insights from the Jeffara escarpment
477 (Libya–Tunisia). *J. Afr. Earth Sci.* 46, pp, 346-370.
- 478 Brunet. M., and Cloetingh. S., 2003. Integrated Peri-tethyan Basins studies (PeriTethys
479 Programme). *Sedimentary Geology* 156. pp 1-10.
- 480 Bumby, A. J., and Guiraud, R., 2005. The geodynamic setting of the Phanerozoic basins of
481 Africa *J. Afr. Earth Sci.* 43. pp, 1-12.
- 482 Burollet. P. F., 1991. Structures and tectonics of Tunisia. *Tectonophysics* 195.P, 359-369.
- 483 Catalano, R., Di stefano, P., Sulli, A., and Vitale, F.P., 1996. Paleogeography and structure of
484 the central Mediterranean: sicily and its offshore area. *Tectonophysics* 260. pp, 291-323.
- 485 Chaabani, F., and Razgallah, S., 2006. Aptian sedimentation: an example of interaction
486 between tectonics and eustatics in Central Tunisia. Geological Society, London, Special
487 Publications, 262. pp, 55-74.
- 488 Courel, L., Aït Salem, H., Benaouiss, N., Et-Touhami, M., Fekirine, B. Oujidi, M., Soussi,
489 M., and Tourani, A., 2003. Mid-Triassic to Early Liassic clastic/evaporitic deposits over the
490 Maghreb Platform. *Palaeogeogr. Palaeoclimatol. Palaeoecol.* 196, 157–176.
- 491 DeCelles, P. G., and K. N. Giles (1996), Foreland basin systems, *Basin Res.*, 8, 105–123,
492 doi:10.1046/j.1365-2117.1996.01491.x.
- 493 Dercourt, J., Zonenshain, L.P., Ricou, L.P., Kazmin, V.G., Le Pichon, X., Knipper, A.L.,
494 Laurier, J.P., Bashenov, M.L., Boulin, J., Pechersky, D.H., Biju Duval, B., Savostin, L.A.,
495 Lepvrier, C., and Geysant, J., 1986. Geological evolution of the Tethys belt from the atlantic
496 to the pamirs since the LIAS. *Tectonophysics* 123 (1-4), 241-315. 15
- 497 Deteil. J., Zouari. H., Chikhaoui. M., Creuzot. G., Ouali. J, Turki M. M., Yaïch. C et
498 Zargouni. F. 1991. Relation entre ouvertures téthysienne et mésogéenne en Tunisie. *Bull.*
499 *Soc.Géol. France*, t. 162, n°6 .p1173-1181.

- 500 Dewey, J.F., Hempton, M. R., Kidd, W. S. F., Saroglu, F., and Segnör, A. M. C., 1986.
501 Shortening of continental lithosphere: The neotectonics of eastern Anatolia. *Special*
502 *Publications Geological Society London* 19, pp 3-36.
- 503 Dhahri, F., and Boukadi, N., 2010. The evolution of pre- existing structures during the
504 tectonic inversion process of the Atlas chain of Tunisia. *J. Afr. Earth Sci.* 56. pp 139–149.
- 505 Doglioni, C., Fernandez, M., Gueguen E and Sabat, F., 1999. On the interference between the
506 early Apennines–Maghrebides back arc extension and the Alps-betics orogen in the Neogene
507 geodynamics of the Western Mediterranean. *Bol. Soc. Geol. Ital.* 118, pp 75– 89.
- 508 Ellouz, N., Patriat, M., Gaulier, J.M., Bouatmani, R., and Sabounji, S., 2003. From rifting to
509 Alpine inversion: Mesozoic and Cenozoic subsidence history of some Moroccan basins.
510 *Sedimentary Geology.* 156, pp 185-212.
- 511 Frizon de Lamotte, D., Leturmy, P., Missenard, Y., Khomsi, S., Ruiz, G., Saddiqi, O.,
512 Guillocheau, F., and Michard, A., 2009. Mesozoic and Cenozoic vertical movements in the
513 Atlas system (Algeria, Morocco, Tunisia): an overview. *Tectonophysics.* 475. pp, 9-28.
- 514 Frizon de Lamotte, D., Michard, A., and Saddiqi, O., 2006. Some recent developments on the
515 geodynamics of the Maghreb. *C. R. Geosciences*, v. 338, 1-10 n° 1-2.
- 516 Gharbi, M., 2008. Étude Tectonique de la région de Zemlet El Beidha (Chaîne Nord des
517 Chotts) : Structuration Crétacée et Evolution Tertiaire. *Mastère Fac Sci. of Tunis University*
518 *Tunis-El-Manar.* 86p.
- 519 Guiraud, R., 1998. Mesozoic rifting and basin inversion along the northern African Tethyan
520 margin: an overview. In: MacGregor, D.S., Moody, R.T.J., Clark-Lowes, D.D. (Eds.),
521 *Petroleum Geology of North Africa.* Geological Society, London, Special Publication 133, pp.
522 217-229.

- 523 Guiraud, R., and Bosworth, W., 1997. Senonian basin inversion and rejuvenation of rifting in
524 Africa and Arabia: synthesis and implications to plate-scale tectonics. *Tectonophysics* 282, pp
525 39-82.
- 526 Guiraud, R., and Bosworth, W., 1999. Phanerozoic geodynamic evolution of northeastern
527 Africa and the northwestern Arabian platform. *Tectonophysics*. 315, pp 73-108.
- 528 Guiraud, R., et Maurin, J.C., 1991. Le rifting en Afrique au Crétacé inférieur: synthèse
529 structurale, mise en évidence de deux étapes dans la genèse des bassins, relations avec les
530 ouvertures océaniques périafricaines. *Bull. Soc. Géol. France* 162, pp 811-823.
- 531 Guiraud, R., and Maurin, J.C., 1992. Early Cretaceous Rifts of Western and Central Africa.
532 An overview. *Tectonophysics* 213, pp 153-168.
- 533 Guiraud, R., and Bosworth, W., Thierry, J and Delplanque, A., 2005. Phanerozoic geological
534 evolution of Northern and Central Africa: An overview *J. Afr. Earth Sci.* 43, pp 83-143.
- 535 Herkat, M., and Guiraud, R., 2006. The relationships between tectonics and sedimentation in
536 the Late Cretaceous series of the Eastern Atlasic Domain (Algeria). *J. Afr. Earth Sci.* 46, pp
537 346-370.
- 538 Hlaïem, A. 1999. Halokinesis and structural evolution of the major features in eastern and
539 southern Tunisian Atlas. *Tectonophysics* 306, pp. 79-95.
- 540 Laridhi-Ouazaa, N., and Bédir, M., 2004. Les migrations tectono-magmatiques du Trias au
541 Miocène sur la marge orientale de la Tunisie. *Africa Geosciences Review*, Vol. II, n°3,
542 pp179-196.
- 543 Laville, E., Pique, A., Amrhar, M., and Charroud, M., 2004. A restatement of the Mesozoic
544 Atlasic Rifting (Morocco). *J. Afr. Earth Sci.* 38, pp 145-153.
- 545 Lazzez, M., and Ben Youssef, M., 2008. Relative Sea-level Changes of the Lower Cretaceous
546 Deposits in the Chotts Area of Southern Tunisia. *Turkish J. Earth Sci.*, 17, pp 835-845.

- 547 Lazzez, M., Zouaghi, T., and Ben Youssef, M., 2008. Austrian phase on the northern African
548 margin inferred from sequence stratigraphy and sedimentary records in southern Tunisia
549 (Chotts and Djefara areas). *C. R. Geosciences*, v. 340. Issue 8, pp 543-555 C.
- 550 Louhaïchi, M. A., et Tlig, S., 1993. Tectonique synsédimentaire des séries post-Barrémiennes
551 au Nord-Est de la chaîne Nord des Chotts (Tunisie méridionale). *Géologie méditerranéenne*.
552 XX, n°1, pp 53-74.
- 553 Marmi, R., and Guiraud, R., 2006. End Cretaceous to recent polyphased compressive
554 tectonics along the “Mole Constantinois” and foreland (NE Algeria). *J. Afr. Earth Sci.* 45, pp
555 123–136.
- 556 Martinez, C., Chikhaoui, M., Truillet, R., Ouali, J., and Creuzot, G., 1991. Le contexte
557 géodynamique de la distension albo-aptienne en Tunisie septentrionale et centrale:
558 structuration éocène de l’Atlas tunisien. *Eclogae Geologicae Helvetiae* 84, pp 61-82.
- 559 Masrouhi, A. and Koyi. H., 2012. Submarine “salt glacier” kinematics of Northern Tunisia, a
560 case of Triassic salt mobility in North African Cretaceous passive margin. *Alsop, G. I.,*
561 *Archer, S. G., Hartley, A., Grant, N. T and Hodgkinson, R. J. Geol. R. (eds) 2012. Salt*
562 *Tectonics, Sediments and Prospectivity. Geological Society, London, Special Publications,*
563 *363, pp 579–593. <http://dx.doi.org/10.1144/SP363.29>.*
- 564 Masrouhi, A., Ghanmi, M., Ben Slama, M.-M., Ben Youssef, M., Vila, J.-M, and Zargouni,
565 F., 2008. New tectono-sedimentary evidence constraining the timing of the positive tectonic
566 inversion and the Eocene Atlasic phase in northern Tunisia: Implication for the North African
567 paleo-margin evolution. *C. R. Geosciences*, 340. pp 771-778.
- 568 Masrouhi, A., Ghanmi, M., Youssef, M.B., Vila, J.M., and Zargouni, F., 2007, Mise en
569 évidence d’une nappe de charriage à deux unités paléogènes au plateau de Lansarine (Tunisie
570 du Nord): Définition d’un nouvel élément structural de l’Atlas Tunisien et réévaluation du
571 calendrier des serrages tertiaires: *C. R. Geosciences*, v. 339, p. 441–448.

- 572 Patriat, M., Ellouz N., Dey Z., Gaulier J. M., and Ben Kilani H., 2003. The Hammamet,
573 Gabes and Chotts basins (Tunisia) a review of the subsidence history. *Sedimentary geology*
574 156, pp 241-262.
- 575 Negra, M. H., Purser, B. H., M'rabet, A. 1995. Sedimentation, diagenesis and syntectonic
576 erosion of Upper Cretaceous rudist mounds in central Tunisia. *Carbonate mud-mounds: their*
577 *origin and evolution*, pp. 401-419.
- 578 Philip, H., Andrieux, J., Dlala, M., Chihi, L., and Ben Ayed, N., 1986. Evolution tectonique
579 moi- plio-quadernaire du fossée de Kasserine (Tunisie centrale): implications sur l'évolution
580 géodynamique récente de la Tunisie. *Bull. Soc. Géol. France*, 8 t. II, 4, 559-568.
- 581 Piqué, A., A Brahim., L., Ait Ouali, R., Amrhar, M., Charroud, M., Gourmelen, C., Laville,
582 E., Rekhiss, F., and Tricart, P., 1998. Evolution structurale des domaines atlasiques du
583 Maghreb au Méso-Cénozoïque; le rôle des structures héritées dans la déformation du domaine
584 atlasique de l'Afrique du Nord. *Bull. Soc. Géol. France*, 6 t. 169, 797-810. pp.217-231.
- 585 Piqué, A., Tricart, P., Guiraud, R., Laville, E., Bouaziz, S., Amrhar, M., and Ait Ouali, R.,
586 2002. The Mesozoic-Cenozoic Atlas belt (North Africa): an overview. *Geodinamica Acta* 15,
587 pp185-208.
- 588 Raulin, C., Lamotte, D.F.D., Bouaziz, S., Khomsi, S., Mouchot, N., Ruiz, G., Guillocheau, F.
589 2011. Late Triassic-early Jurassic block tilting along E-W faults, in southern Tunisia: New
590 interpretation of the Tebaga of Medenine. *Journal of African Earth Sciences* 61, pp. 94-104
- 591 Rigane, A., Feki, M., Gourmelen, C., and Montacer, M., 2010. The "Aptian Crisis" of the
592 South-Tethyan margin: New tectonic data in Tunisia. *J. Afr. Earth Sci.* 57. pp. 360-366.
- 593 Souquet, P., Peybernès, B., Saadi, J., BenYoussef, M., Ghanmi, M., Zarbout, M., Chikhaoui,
594 M., and Kamoun, F., 1997. Séquences et cycles d'ordre 2 en régime extensif et transtensif:
595 exemple du Crétacé inférieur de l'Atlas tunisien, *Bull. Soc. geol. France* 168, pp. 373-386.

- 596 Soyer, C. and Tricart, P., 1987. La crise aptienne en Tunisie centrale : approche
597 paléostrutturale aux confins de l'Atlas et l'Axe Nord-Sud. C.R. Acad. Sci. Paris. t. 305 (Serie
598 II), pp. 301–305.
- 599 Vergès, J. and Sabàt, F., 1999. Constraints on the western Mediterranean kinematics evolution
600 along a 1000 km transect from Iberia to Africa. In: Durand, B. (Ed.). The Mediterranean
601 Basins: Tertiary Extension within the Alpine Orogen, vol. 156. Geol. Soc. Spec. Publ.,
602 London, pp. 63–80.
- 603 Vially, R.; Letouzey, J.; Bernard, F.; Haddadi, N.; Desforges, G.; Askri, H. and Boudjema, A.,
604 1994. Basin inversion along the northern African margin: the Saharan Atlas (Algeria). In:
605 Peri-Tethyan Platforms, F. Roure (Ed.), pp. 79-118, Edition Technip, Paris.
- 606 Zargouni, F., 1984. Style et chronologie des déformations des structures de l'Atlas tunisien
607 méridional. Évolution récente de l'accident Sud-atlasique. C.R. Acad Sc.Paris, t.299, Série II,
608 n°2. pp.179-196.
- 609 Zargouni, F., 1985. Tectonique de l'Atlas méridional de Tunisie, évolution géométrique et
610 cinématique des structures en zone de cisaillement. Thèse d'Etat, Univ. Louis Pasteur,
611 Strasbourg-Paris.
- 612 Zargouni, F., Rabiaa, M.C., et Abbès, C., 1985. Rôle des couloirs de cisaillement de Gafsa et
613 de Négrine-Tozeur dans la structuration du faisceau des plis des Chotts, éléments de l'accident
614 sud-atlasique. C.R. Acad Sc.Paris, t 301. 11, pp. 831-883.
- 615 Zghal, I, Ouali, J, et Bismuth, H. 1998. Syn-sedimentary tectonics in central Tunisia (Jebel
616 Mrhila area) during the Aptian-Albian. C.R. Acad Sc Paris, V 326, 3, pp 187-192.
- 617 Zouaghi, T., Bédir, M., and Inoubli, M, H., 2005. 2 D Seismic interpretation of strike-slip
618 faulting, salt tectonics, and Cretaceous unconformities, Atlas Mountains, central Tunisia. J.
619 Afr. Earth Sci. pp. Vol. 43, pp 464-486.

620 Zouaghi, T.; Ferhi, I.; Bédir, M.; Ben Youssef, M.; Gasmi, M. and Inoubli, M.H., 2011.
621 Analysis of Cretaceous (Aptian) strata in central Tunisia, using 2D seismic data and well logs.
622 . Afr. Earth Sci. Vol. 61, pp. 38-61.
623 Zouari, H., Turki, M.M., Delteil, J., et Stephan, J.-F., 1999. Tectonique transtensive de la
624 paléomarge tunisienne au cours de l'Aptien-Campanien. Bull. Soc. Géol. France 170 (3), pp.
625 295–301.

626 **Figure captions**

627 **Figure 1:** Structural map of the northern African margin. B. Tectonic background of the
628 southern Atlas of Tunisia is mapped based on satellite images analysis and field investigations
629 (The base map is produced using elevation data from NASA SRTM Gtopo 30). C. Geological
630 map of the North Chotts range with the location of Zemlet el Beidha.

631 **Figure 2:** Detailed geologic map of the Zemlet el Beidha anticline. Location of Fig. 5 is
632 shown. The cross sections A-A' and B-B' are located in Fig. 4.

633 **Figure 3:** Stratigraphic column of the Mesozoic and Cenozoic series in the Zemlet el Beidha
634 region. Only the outcropping series are shown.

635 **Figure 4:** Surface cross sections (For location, see Fig. 2) across the Zemlet El Beidha
636 anticline. Section A-A' demonstrates the reactivation of the normal fault as reverse fault in the
637 east of Tebaga Fatnassa structure. Section (B-B') shows the role of the NW-SE strike slip
638 fault of the Fejej system (Fig. 2) affecting the southwestern part of Zemlet el Beidha.

639 **Figure 5:** A: The SPOT image of the Khanguet Aïcha area; B: Interpretative geological and
640 structural map of Khanguet Aïcha area; C: The correlation of Barremian deposits with the
641 normal fault of Khanguet Aïcha; D: Lower hemisphere stereographic projection of planes and
642 striations of the Khanguet Aïcha and Khanguet Amor faults. The back-tilting shows the
643 existent N100-110° E trending normal fault of Khanguet Aïcha and Khanguet Amor.

644 **Figure 6:** A: Panoramic view of the tilted synsedimentary Khanguet Aicha normal fault. This
645 fault affects the Sidi Aïch and Orbata Formations and is sealed by the Coniacian-Santonian
646 strata. B: Photograph of the tilted Khanguet Amor normal fault associated with syntectonic
647 conglomerates of the Orbata Formation.

648 **Figure 7:** Details of the Aptian syn-tectonic conglomerates of the Orbata Formation.
649 A: The Aptian conglomerate; B: The metric bed of Aptian conglomerates located in the
650 Khanguet Amor (See fig. 2); C and D: Small conglomerates resedimented in the Khanguet
651 Aicha and Khanguet Amor.

652 **Figure 8:** Panoramic view, looking ENE, of a preserved Early Cretaceous normal fault. For
653 location, see Fig. 2 Growth strata located in the hanging-wall indicate that this normal fault
654 was active at least during the Albian.

655 **Figure 9:** Shortcut inverted normal fault with hangingwall shortcut deformation in the
656 Bouhedma Formation.

657 **Figure 10:** A: NE-SW correlations of Cretaceous sedimentary log in the Zemlet el Beidha
658 This correlation shows evidence of a central horst (Zemlet el Beidha) and lateral grabens
659 (Fejej and Romana). Note the major thickening of the Cretaceous sediments toward the major
660 faults. B: Block diagram showing tilted half graben systems of the Zemlet el Beidha as a
661 result of a N to NE extension during Aptian-Albian(see Fig.5 D).

662 **Figure 11:** Photographs showing the principal features of the extensional Cretaceous along
663 the Zemlet el Beidha structure. (A) The olistholites within the Bouhedma Formation indicate
664 the depositional syn-rift. (B) Conglomerate interstratified in the Bouhedma Formation. (C)
665 Ammonite Aptian in the Orabata Formation. (D) Rudist fossils (arrows) within the Aleg
666 Formation (Coniacian-Santonian).

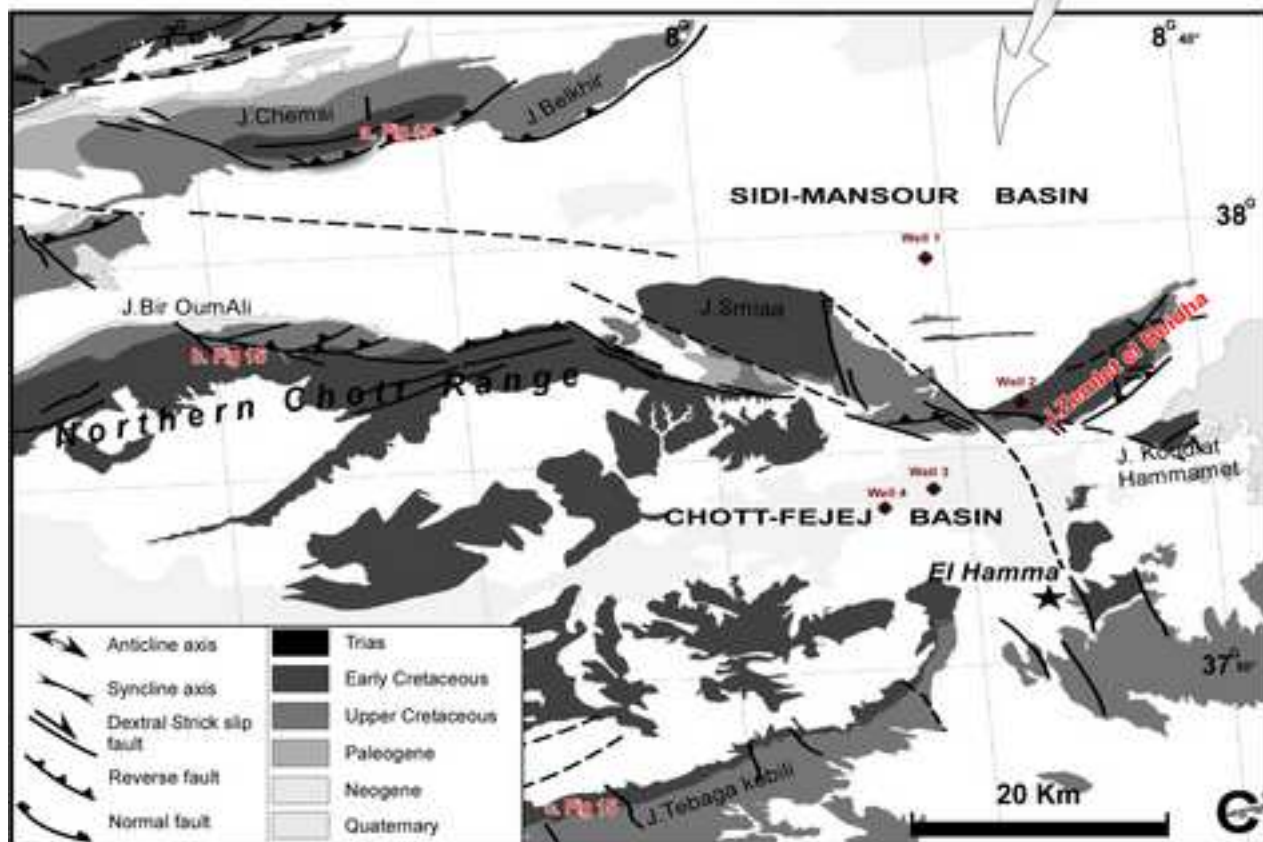
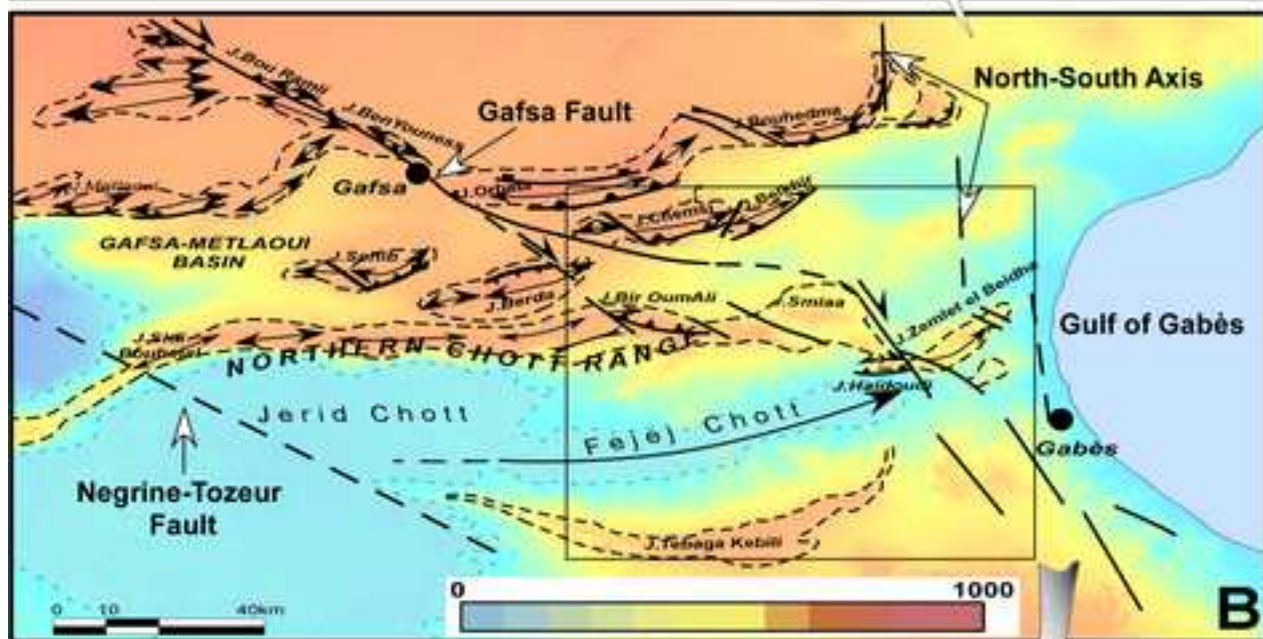
667 **Figure 12:** Seismic reflexion profiles EL05 and EL07 across the Sidi Mansour Basin,
668 showing horst and graben systems trending NNE–SSW related to the extension of the

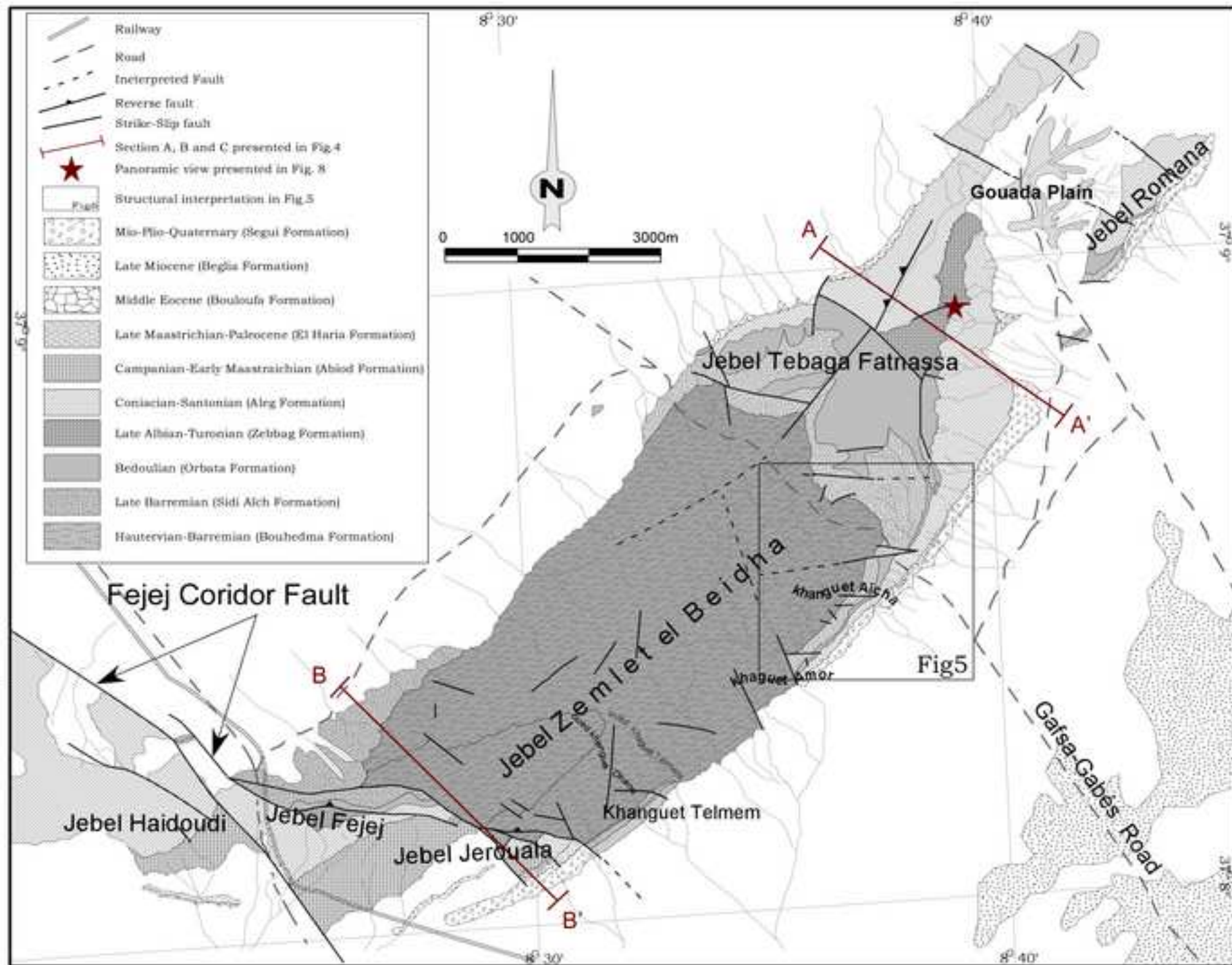
669 Tethyan margin. The base map is produced using elevation data from NASA SRTM Gtopo
670 30 shows the position of seismic sections and the locations of petroleum wells used in this
671 study.

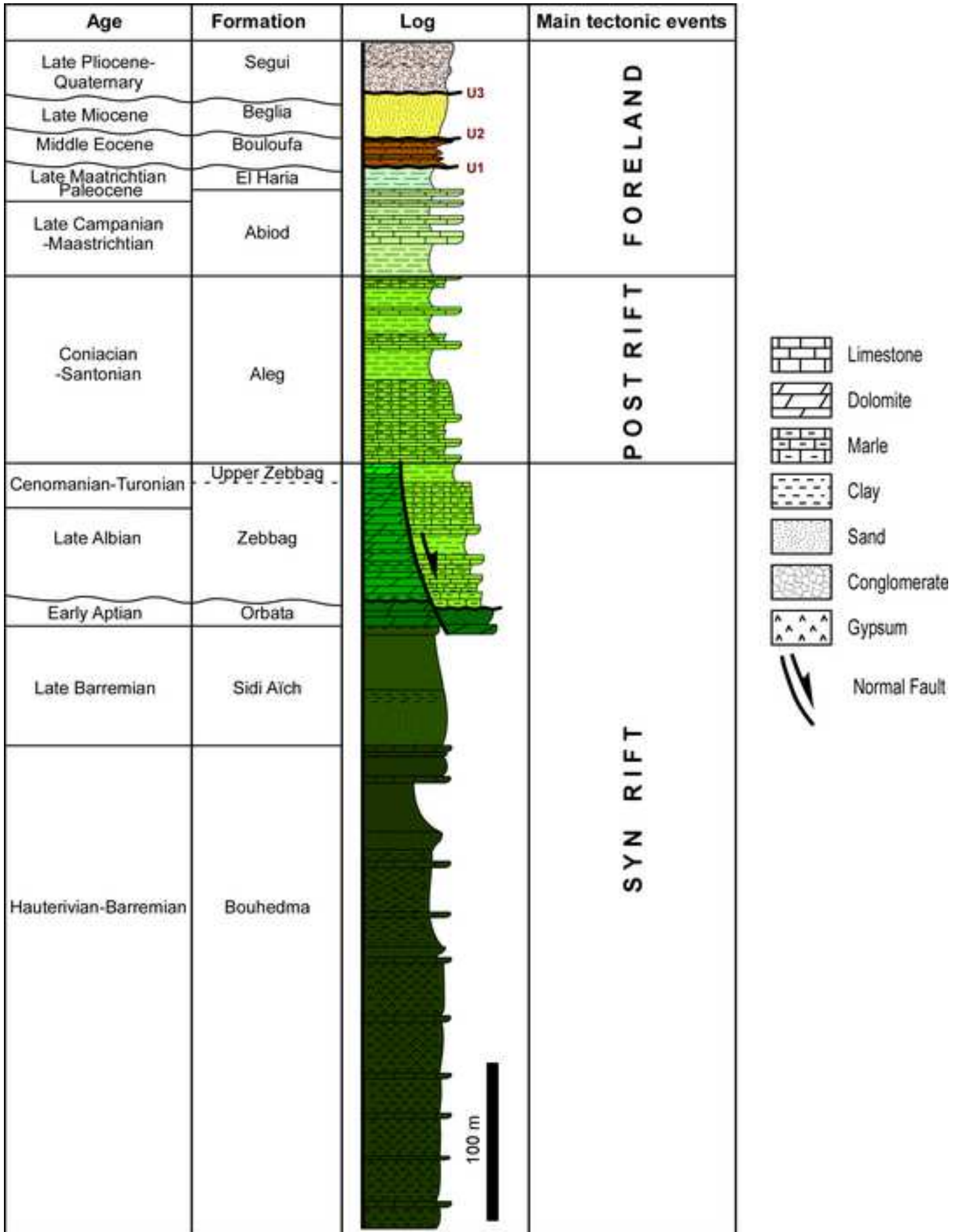
672 **Figure 13:** Interpretative model of Khanguet Aicha fault: genetic mechanism explaining the
673 presence of sedimentary discontinuity ds1 and ds2 of the upper Aptian and Early Albian
674 deposit related to extensional tectonic. See details in the text.

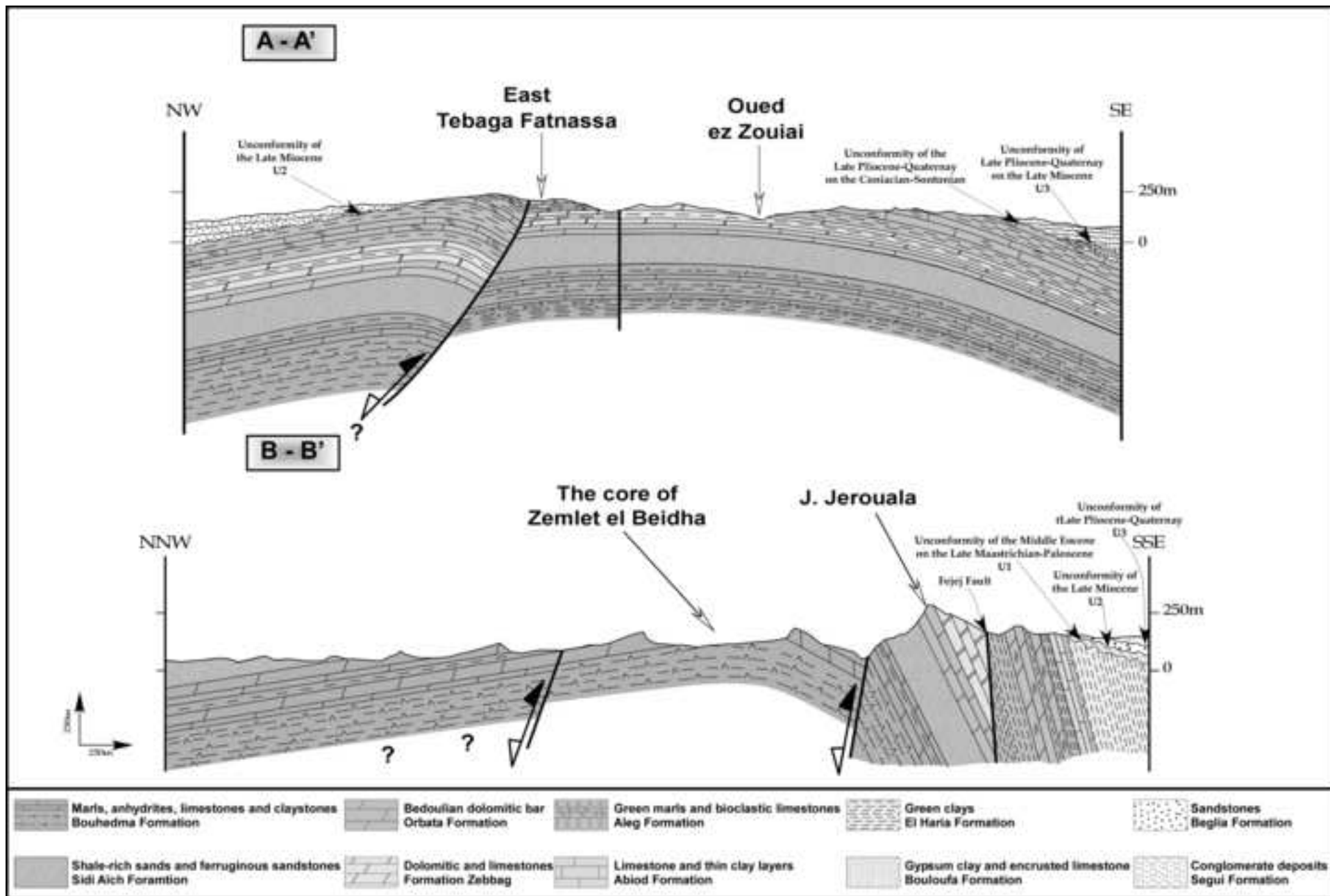
675 **Figure 14:** Similar Aptian-Albian extensional structures observed in the southern Atlas of
676 Tunisia. A: The core of the Chemsî anticline shows, still preserved, a normal fault affecting
677 the Albian series; B: Graben in the Aptian series; C: Map view (Google Earth image) of the
678 Jebel Tebaga of Kebili. The geological interpretation shows that the Orbata Formation is
679 affected by the normal fault, sealed by the Zebbag Formation.

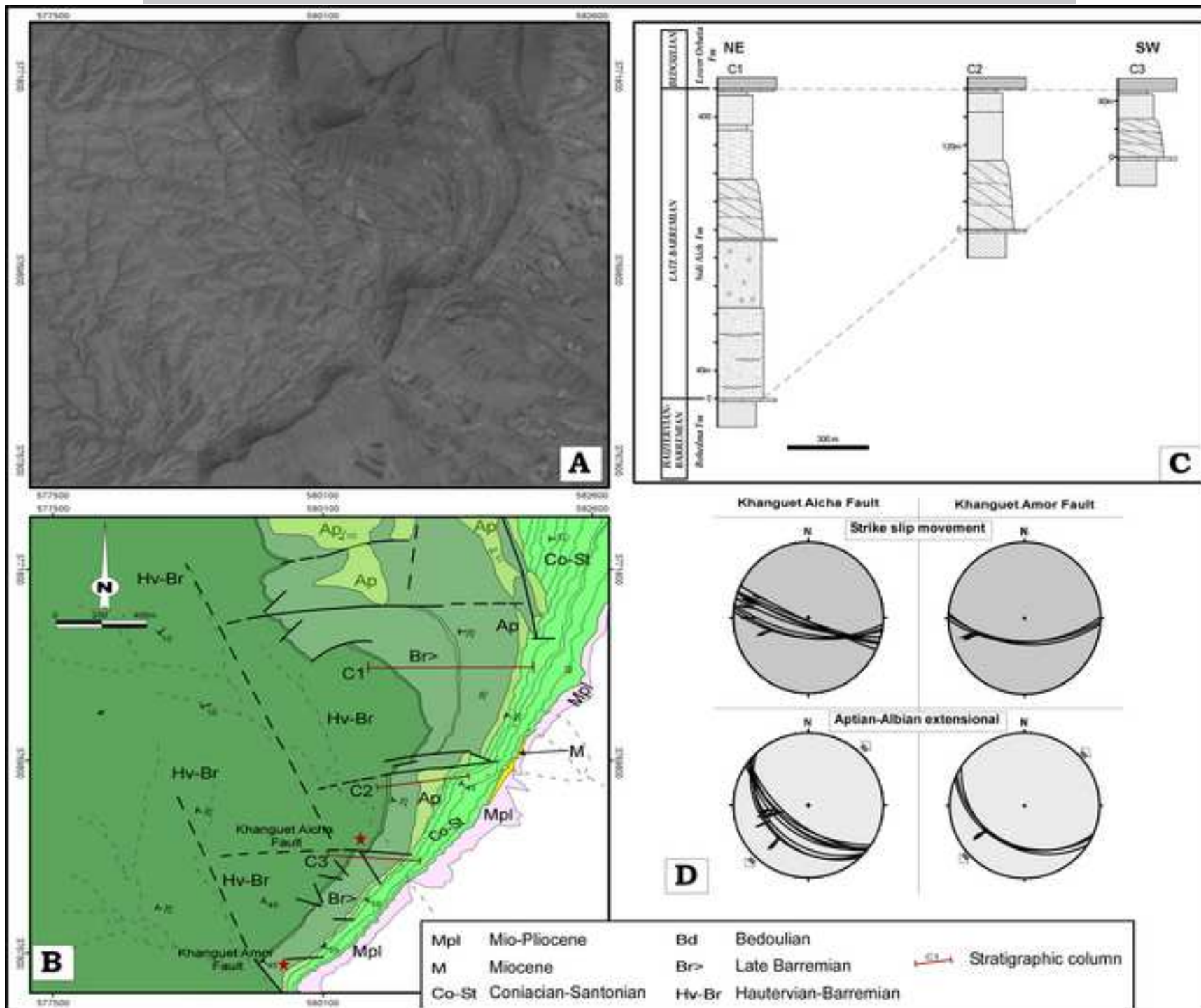
680 **Table 1:** Biostratigraphic data from the Zemlet el Beidha. Location of sample are in meter
681 (UTM system). Microfauna and corresponding age of samples are also shown.

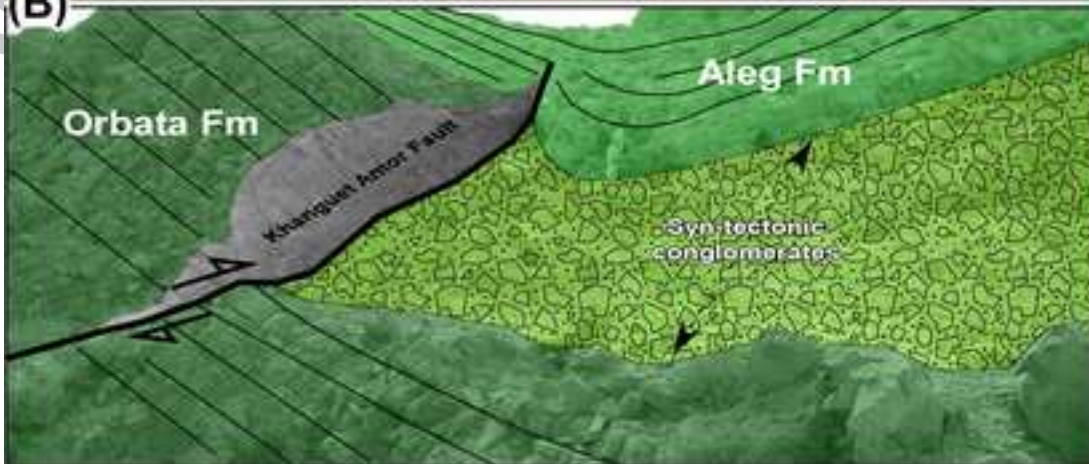
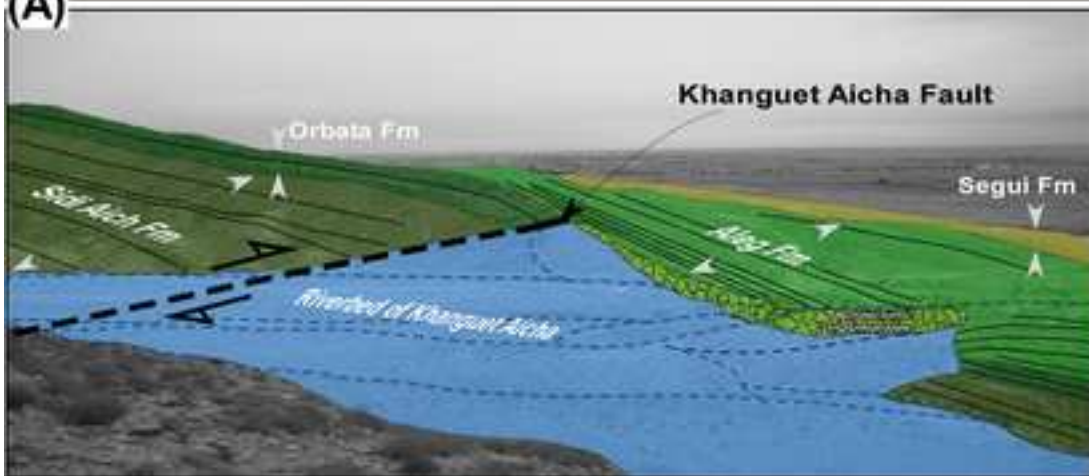




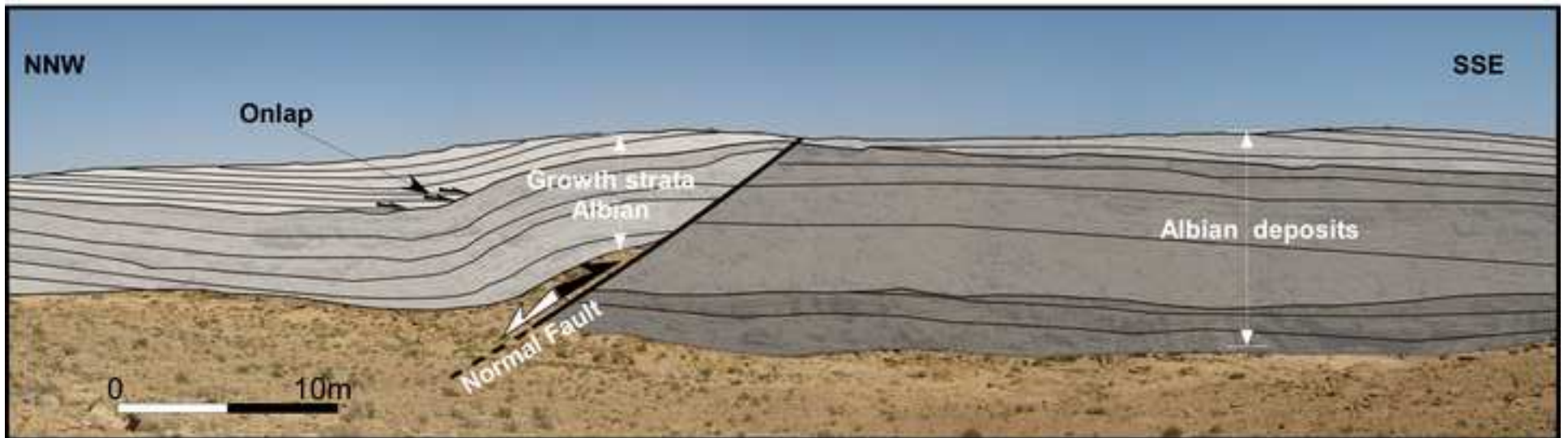


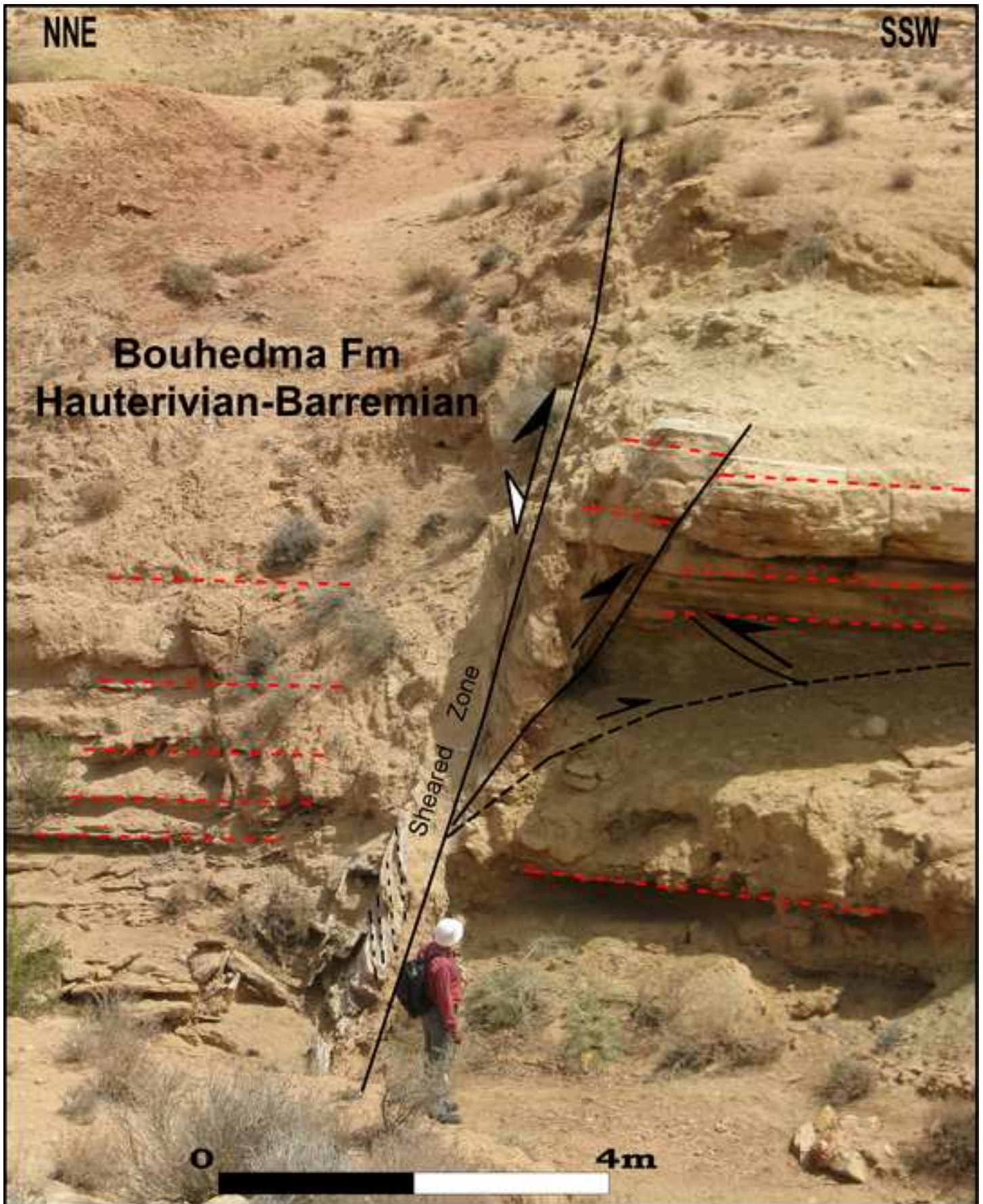


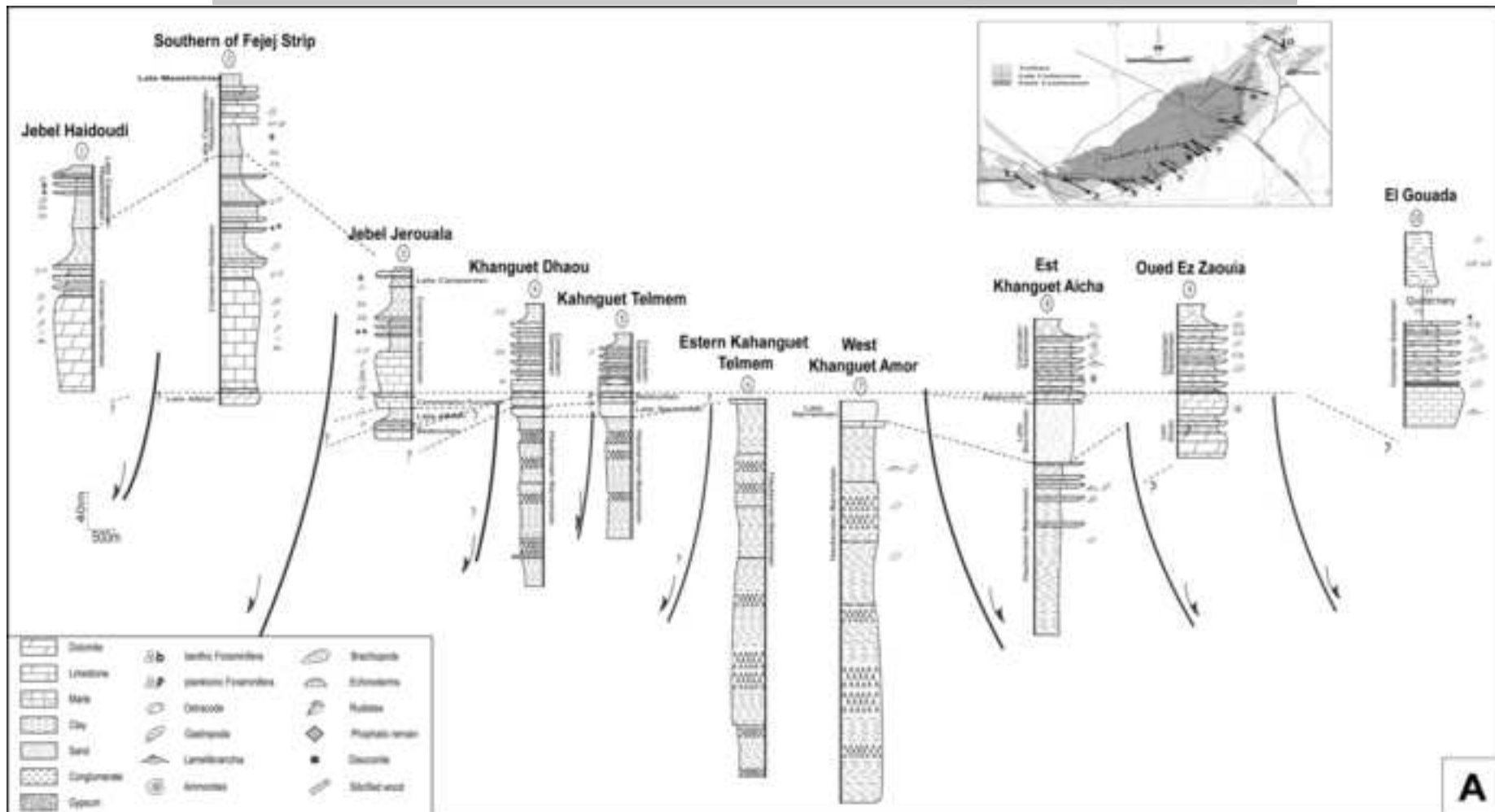




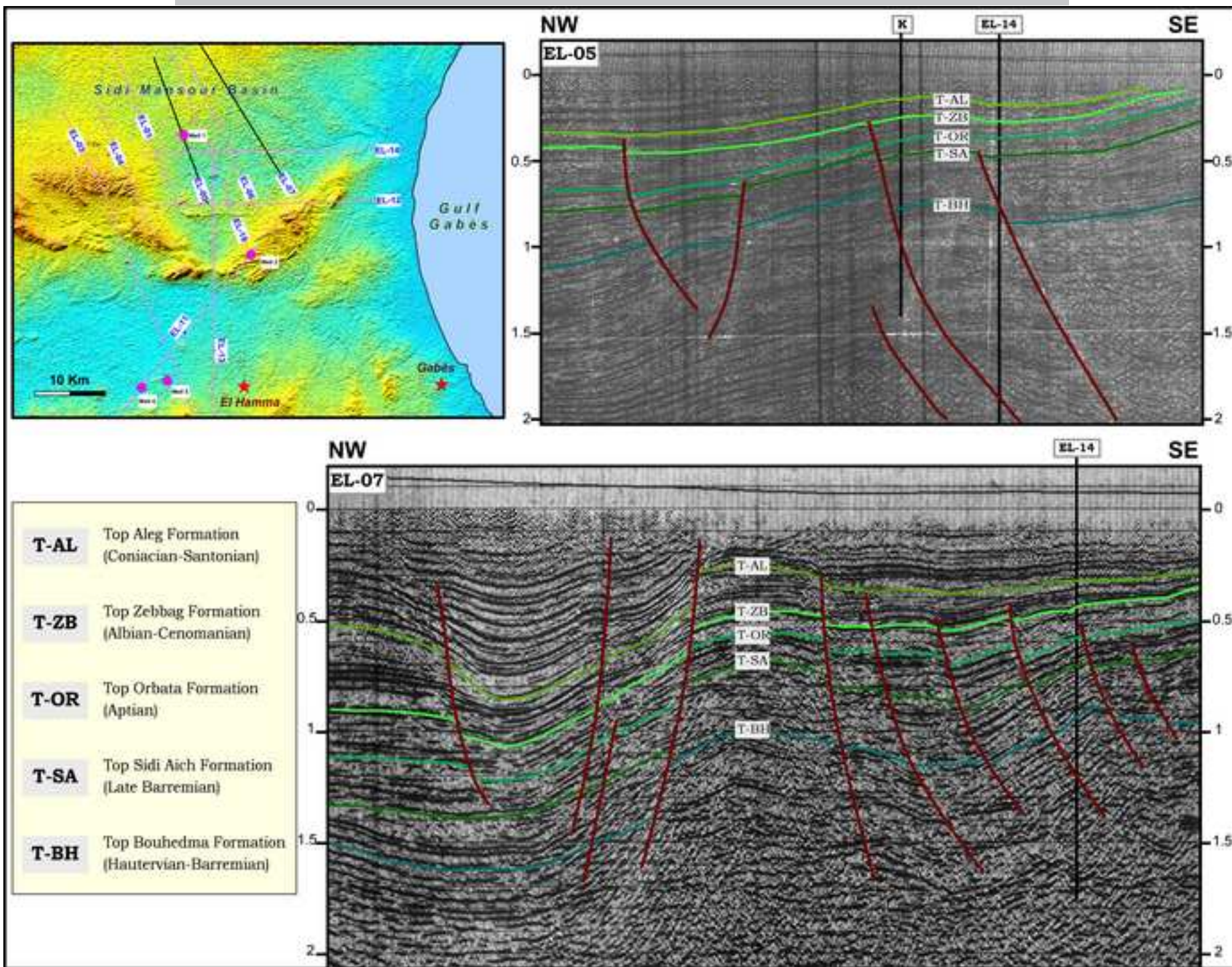


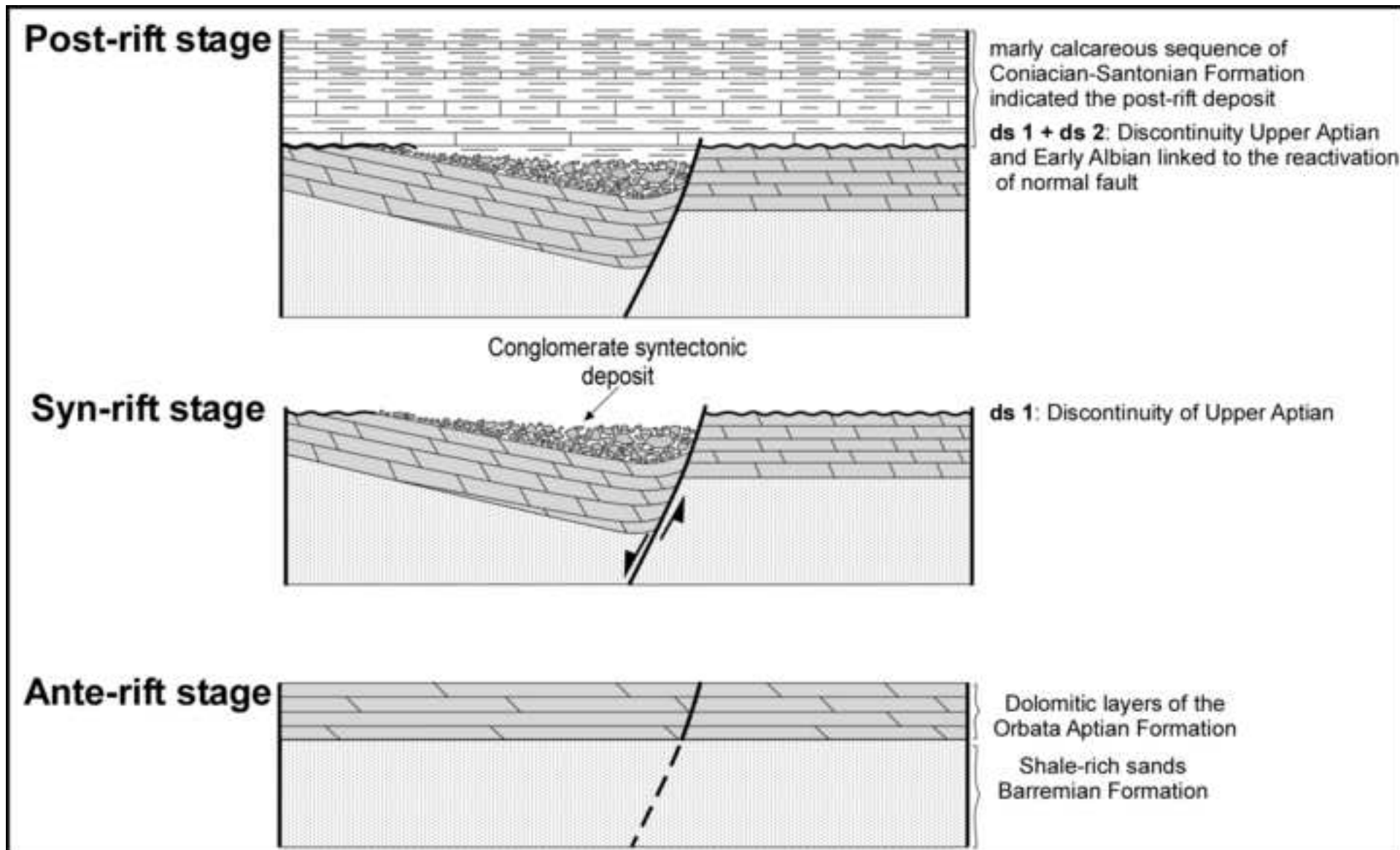


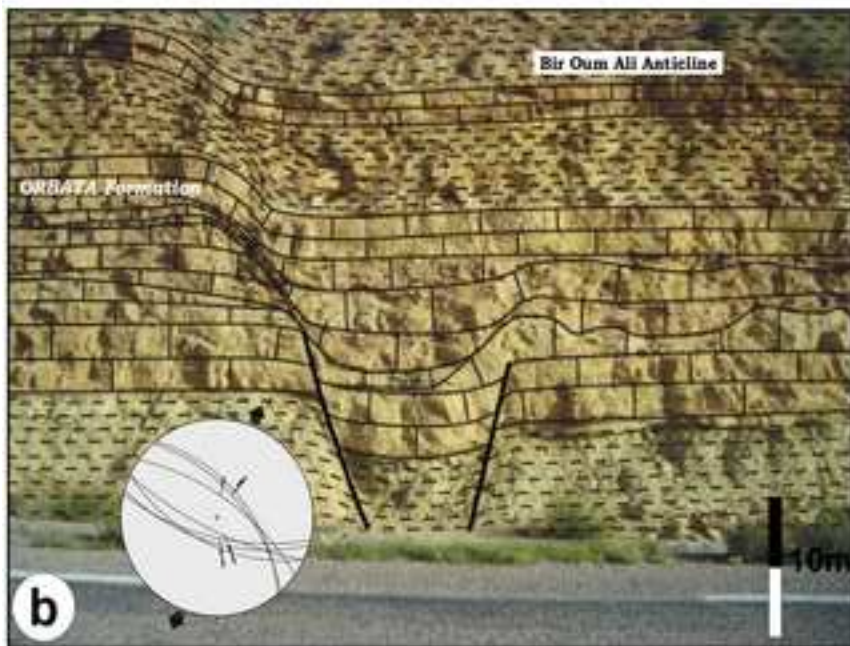
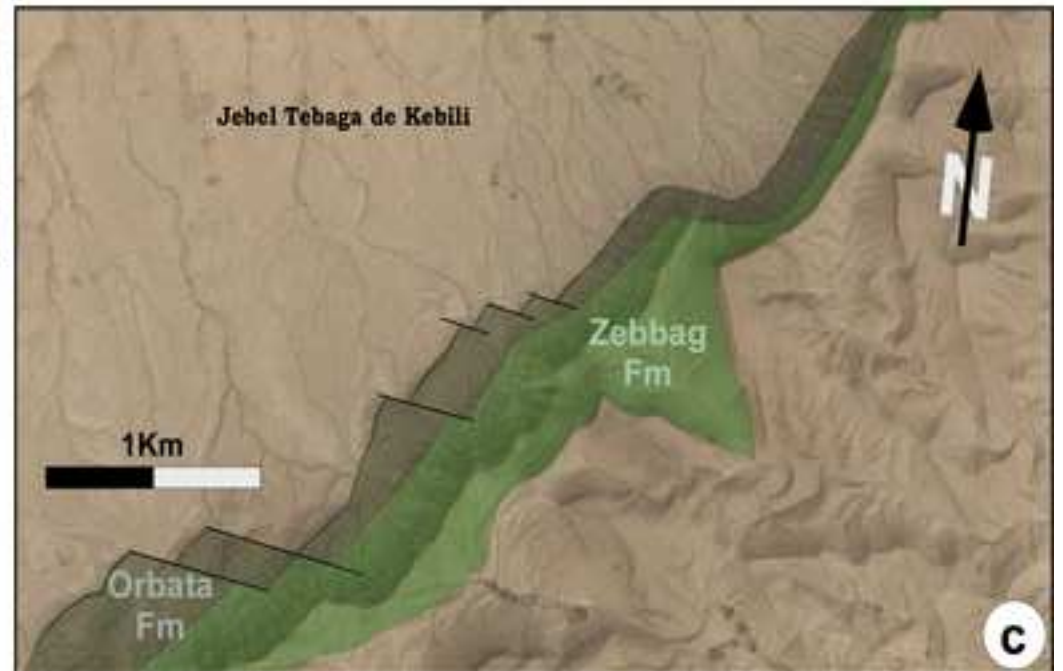
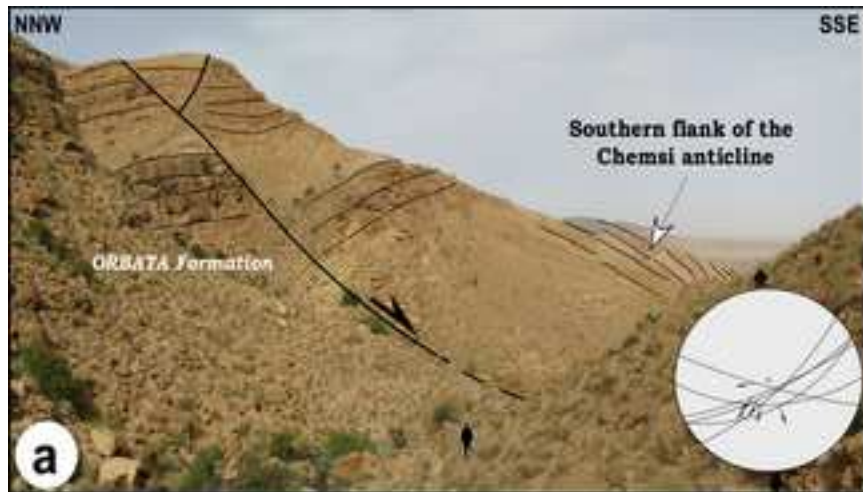












Locality	Nb	X	Y	Fauna	Age
Jebel Romana-Gouada plain	EH 152	585047	3,775,657	<i>Echinoderme, Cytherella sp, Cythereis sp, Brachycythere</i>	Coniacian-Santonian
	EH 153	585000	3,775,593	<i>Radiole, Cytherella sp, Bairdia sp</i>	Coniacian-Santonian
	EH 155	584483	3,775,204	<i>Rotallia, Gavelinella sp, Lenticulina sp.</i>	Coniacian-Santonian
	EH 156	582497	3,775,659	<i>Rotallia, Gavelinella sp</i>	Coniacian-Santonian
	EH 220	584,262	3,774,591	<i>Brachycythere, Globotruncana fornicata, Bairdia sp.</i>	Coniacian-Santonian
	EH 221	584,257	3,774,589	<i>Globotruncana fornicata, Globigerinelloides aspera, Lenticulina.</i>	Coniacian-Santonian
Tebaga Fatnassa-Oued ez Zouaia	EH 118	580,635	3,774,718	<i>Ammonites, Cytherella sp, Bairdia sp,</i>	Coniacian-Santonian
	EH 124	581,839	3,773,088	<i>Ammonites, Brachycythere, Bairdia sp,</i>	Coniacian-Santonian
	EH 125	581,752	3,773,090	<i>Ammonites, Echinodermes, Ostreas, Cytherella sp.</i>	Coniacian-Santonian
	EH 128	581,199	3,773,404	<i>Dawinula sp, Cythereis sp</i>	Late Albian
	EH 130	578,345	3,773,830	<i>Radiole, Ammonites, Brachycythere.</i>	Barremian
Khanguet Aicha-khanguet Amor	EH 113	579,411	3,770,340	<i>Cypridea, Cytherella, Choffatella decipiens</i>	Barremian
	EH 131	577,676	3,768,980	<i>Fabanella, Cypridea, Choffatella decipiens, Fabanella sp, Perissocytheridea</i>	Barremian
	EH 173	580,877	3,769,897	<i>Cytherella dextrocephematta, Numidica, Cytherella</i>	Coniacian
	EH 176	580,934	3,769,897	<i>Echinoderme, Cytherella sp, Cythereis sp, Brachycythere</i>	Coniacian-Santonian
	EH 142	571,821	3,766,103	<i>Rotalia, Protobontomia numidica, Gavelinella sp, Globotruncana lapparenti.</i>	Coniacian-Santonian
Jebel Jerouala Khanguet Telmem-khanguet Dhaou	EH 143	571,841	3,766,101	<i>Brachycythere, Cytherella.</i>	Coniacian-Santonian
	EH 145	572,474	3,765,998	<i>Knemiceras, Darwinula sp, pracypris sp</i>	Late Albian
	EH 183	573,864	3,765,434	<i>Cythereis sp, Spiroplectamira sp, Lenticulina sp, Globotruncana arca, Orbitoides.</i>	Late Campanian
	EH 184	573,956	3,765,399	<i>Hedbergella sp, Nodosaria sp, Globotruncana fornicata, Pseudotextularia nutalli.</i>	Late Campanian-Maastrichian
	EH 185	574,019	3,765,358	<i>Protobontonia sp, Hedbergella, Textularia.</i>	Coniacian
	EH 226	575,959	3,765,811	<i>Rudiste.</i>	Turonian
	EH 196	574,228	3,765,587	<i>Cytherelle, Radiole, Ostrea</i>	Coniacian
Jebel Fejej	EH 104	567,146	3,768,270	<i>Echinoderme, Ammonites</i>	Coniacian
	EH 107	568,910	3,765,986	<i>Vaginulopsis sp, Globotruncana arca,</i>	Late Campanian
	EH 109	568,457	3,766,134	<i>Globotruncana rugosa, Macrocypris sp, Globotruncana fornicata.</i>	Late Campanian-Maastrichian
	EH 140	570,900	3,765,808	<i>Echinoderme, Cytherella sp, Cythereis sp, Brachycythere</i>	Late Campanian-Maastrichian
	EH 142	570,926	3,765,758	<i>Globotruncana fournicata, Globigerinelloides aspera, Lenticulina.</i>	Coniacian-Santonian
South Jebel Haidoudi	EH 143	570,999	3,765,737	<i>Rotallia, Gavelinella sp, Lenticulina sp, Brachycythere.</i>	Coniacian-Santonian
	EH 200	568,491	3,765,622	<i>Globotruncana, Lenticulina</i>	Coniacian-Santonian
	EH 201	568,431	3,765,659	<i>Echinoderme, Cytherella sp, Cythereis sp, Brachycythere</i>	Coniacian-Santonian
	EH 202	568,484	3,765,108	<i>Hedbergella sp, Globotruncana fornicata, Pseudotextularia nutalli, Vaginulopsis sp.</i>	Late Campanian-Maastrichian
	EH 207	568,356	3,764,916	<i>Subbotina triloculinoides, Gavelinella danica, Bairdia sp, Globotruncana fornicata.</i>	Paleocene?

684

685 **Highlights:**

686 ▶ We used new data to examine inheritance Cretaceous structure pattern of Atlantic front.

687 ▶ Most faults were active during Aptian – Albian times of rifting stage.

688 ▶ Lower Cretaceous rifting structure are sealed by Coniacian – Santonian post-rift deposits.

689

ACCEPTED MANUSCRIPT